Text and references to accompany Nevada Bureau of Mines and Geology Map 133

GEOLOGIC MAP OF THE SOUTHERN SAND SPRINGS RANGE

CHURCHILL AND MINERAL COUNTIES, NEVADA

by

Joseph I. Satterfield

INTRODUCTION

Setting

The Sand Springs Range (SSR) is a small mountain range (60 km long, 10–15 km wide, 2,600 feet maximum vertical relief) in Churchill and Mineral Counties, west-central Nevada. This map covers the southern SSR, including the southern part of the Sand Springs pluton, a large Cretaceous granitoid (fig. 1). The map area contains a large expanse of pre-Cretaceous rocks, the primary focus of mapping. Pre-Cretaceous rocks include diverse sedimentary, intrusive igneous, and extrusive igneous rocks deformed and metamorphosed to widely varying degrees. With one exception, Cretaceous-Jurassic porphyritic basalt, exposed only in the northern SSR (fig. 1), pre-Cretaceous rocks are metamorphic tectonites. Cretaceous granitoid plutons intrude tectonites throughout the map area; the Sand Springs pluton and the Nevada Scheelite pluton are labeled on the map and on figure 1. Cenozoic intrusive igneous rocks, extrusive igneous rocks, and sediments crop out over large areas on the flanks of the SSR. Cenozoic faults, including range-front faults active in the Quaternary, border and segment much of the range.

The SSR lies within the Mesozoic marine province of the northwestern Great Basin. Rocks of the Mesozoic marine province, exposed in numerous mountain ranges in western Nevada, were deposited in a backarc basin east of the Sierran arc (Speed, 1978; Oldow, 1984). This backarc basin was the site of marine deposition from the Early Triassic into the mid-Jurassic: carbonate and craton-derived siliciclastic sediments were deposited on its eastern flanks, while volcanic rocks, volcanogenic sediments, and interstratified carbonate sediments were deposited to the west. A wide range of depositional environments from intertidal-supratidal to deep basinal have been documented in Triassic and Early Jurassic rocks in various parts of the Mesozoic marine province (Oldow, 1984; Oldow and others, 1993, Stewart, 1997). In the mid-Jurassic through the Early Cretaceous, the Mesozoic marine province was complexly deformed during a protracted history of regional shortening, probably in a transpressional setting in which strike-slip faults and large-displacement thrust faults were active at the same time (e.g., Oldow, 1984).

Major Mesozoic Structural Divisions

In the SSR three generations of Mesozoic structures are distinguished by direct superposition and are designated D_1, D_2, and D_3 from oldest to youngest. Map-scale and outcrop-scale folds and faults are associated with each phase except D_3, which lacks documented faults. A widespread penetrative foliation, S_1, is parallel to D_1 axial planes. The fundamental Mesozoic structural units in the southern SSR are the upper plates of nine mapped or inferred D_2 thrust faults. These upper plates, termed “nappes,” are designated from structurally lowest to highest, n1 to n8 (fig. 2, on plate). The inferred thrust fault at the base of n7 is interpreted to be down-dropped by a Cenozoic high-angle fault and not exposed at the surface (cross sections D–D', E–E'). The structural position of the small exposure of n9 at the eastern margin of the map is not known.

Each D_2 nappe contains up to six Mesozoic fault blocks bounded by faults active during D_1. Where D_1 fault blocks are exposed, they are designated by an a–f within each numbered D_2 nappe. As an example, n2 contains a single D_1 fault separating n2 into two D_1 fault blocks designated n2a and n2b (fig. 2). When upper and lower plates of typically steep D_1 faults can be distinguished, earlier letters of the alphabet signify structurally lower D_1 fault blocks. Fault block boundaries are speculative where covered by post-D_1 units. In the explanation and elsewhere in this paper the structural framework shown on figure 2 is used to describe the locations of map units and key exposures. Evidence supporting this arrangement of faults is summarized in the section on Mesozoic structures.

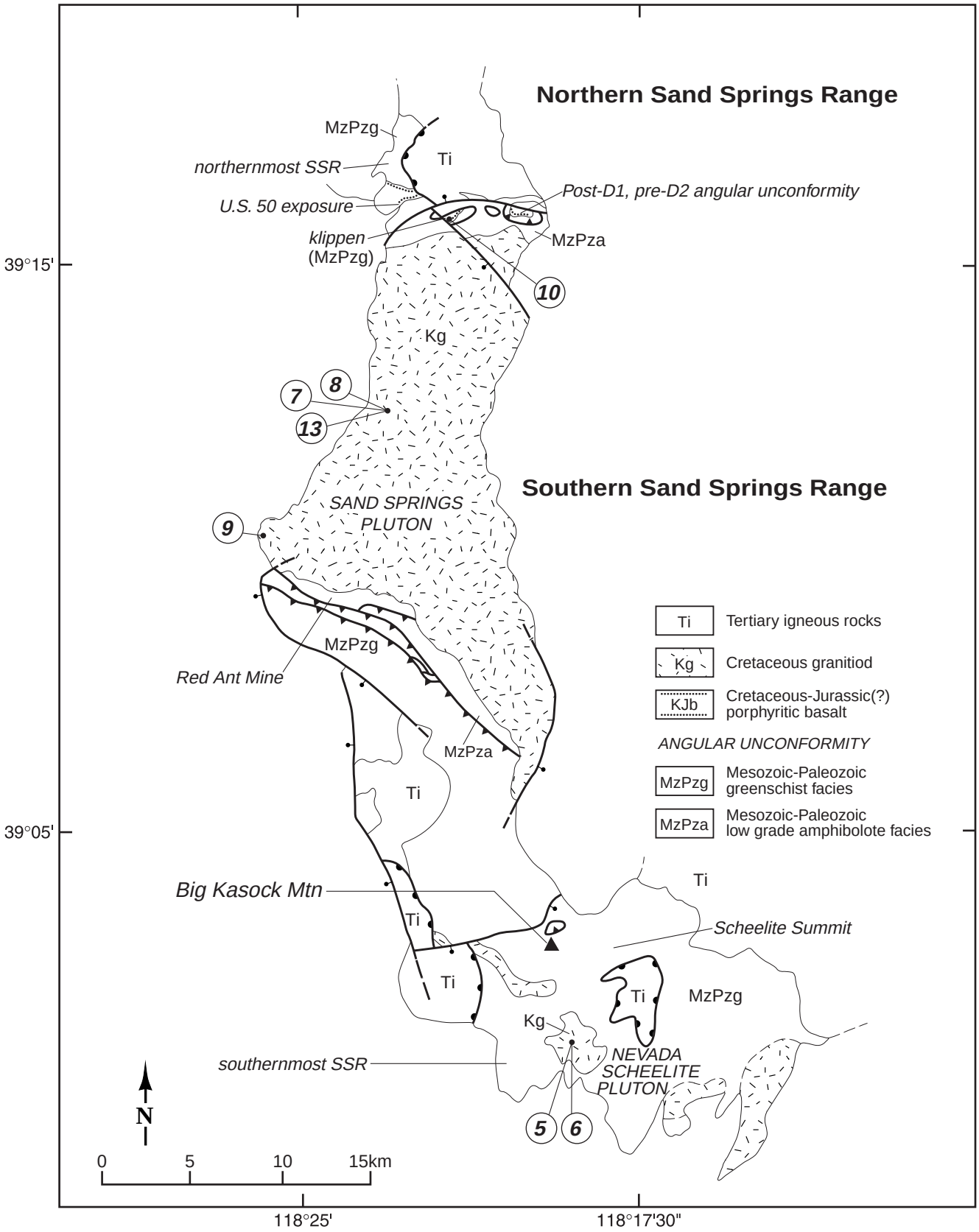

Figure 1. Simplified geologic map of Sand Springs Range showing location of the southern Sand Springs Range, northern Sand Springs Range, and key localities mentioned in text. Locations of isotopic date samples that fall outside the southern Sand Springs Range and locations of dated samples reported in Schilling (1964) are shown as circles. Dates are listed in table 1.

Previous Mapping

Some southern SSR structures and lithologic units have been previously mapped at smaller scales or in small areas of tungsten mineralization. Beal and others (1964) and Schilling (1964) summarized the geology of the SSR and described details of Cretaceous granitoids. Banaszak (1969) prepared a 1:31,600-scale map of the southern SSR and described structures and rock types within. The 1:250,000-scale geologic map of Churchill County covers much of the range and accompanying text includes brief descriptions of structures and rock types in the SSR (Willden and Speed, 1974). The 1:250,000-scale Mineral County geologic map (Ross, 1961) includes the Nevada Scheelite Mine and the southernmost SSR. Most of the SSR lies within the 1:250,000-scale geologic map of the Reno 1° x 2° Quadrangle (Greene and others, 1991). Areas directly adjacent to this map of the southern SSR were mapped or described in Ekren and Byers (1986), Black and others (1991), and Henry (1996). This map confirms approximate locations of many previously mapped contacts, but shows some of these to be of different kind, such as being intrusive or fault contacts rather than depositional. Relative timing relations inferred from this map also differ from some previous interpretations. While Banaszak (1969) and Willden and Speed (1974) interpreted much of the deformation and metamorphism near the Cretaceous Sand Springs pluton to be caused by its forceful intrusion, relations on this map support the hypothesis that Cretaceous pluton emplacement postdated all major phases of Mesozoic deformation.

Significance

The geologic map and accompanying paper present detailed descriptions of rock types and structures in the southern SSR, plus first-order interpretations of contact types and relative timing of geologic events. This information can be applied to several problems. First, the SSR contains particularly well-exposed and abundant folds and faults that can be used to test the several contrasting tectonic models proposed to explain deformation of this part of the Mesozoic marine province (e.g., Speed, 1978; Oldow, 1984; Schweickert and Lahren, 1990; Wyld and others, 1996, 2001). Second, the southern SSR contains extensive exposures of previously little-known pre-Cenozoic rocks. Descriptions of these rocks can be used to help assemble the stratigraphy and paleogeography of this part of the Mesozoic marine province. Third, the SSR contains extensive, well-exposed pluton-country rock contacts and their environs useful for evaluating models of pluton emplacement. Fourth, this map shows the structural and stratigraphic setting of numerous mines and prospects, including the Nevada Scheelite Mine. Regional implications of structures, rock types, contact types, and mine locations in the SSR are not discussed in this paper. This map provides data and first-order interpretations that any regional model must consider.

CENOZOIC GEOLOGY

Rock Types

Unmetamorphosed Cenozoic rocks are subdivided into seven igneous and six sedimentary map units that primarily crop out in downthrown fault blocks along the eastern and western flanks of the range. The ostensibly oldest Cenozoic unit, dark red feldspar porphyry (Tbs), is found in small exposures on the eastern and western margins of the range. Rhyolite intrusive rocks and crystal-lithic tuff (Tr), the most extensively exposed Tertiary unit, includes crystal-lithic tuff containing abundant flattened pumice shards (Trt) as well as quartz-feldspar-biotite porphyry containing intrusive contacts (Tri). Locally boundaries between tuff and intrusive subdivisions of Tr are complex and difficult to locate and as a result are not distinguished everywhere on the map. In the western portion of the map Tr surrounds four ≤0.6 km-long inclusions of Mesozoic and/or Paleozoic carbonate rocks. Mesozoic S_1 orientations within inclusions are consistent with S_1 in adjacent, more continuous tectonite exposures, suggesting inclusions have not been detached or offset from the country rock of Tr. Porphyritic andesite (Ta) overlies Tr and caps one ridge in the southern SSR. Correlative andesite caps mesas in the Cocoon Mountains to the west and in the northern Sand Springs Range and southern Stillwater Range to the north. Its horizontal basal contact in the southern SSR is an angular unconformity above tilted compaction foliation in Tr. Cobble conglomerate (Tcg) and flow breccia (Tvb) are exposed in small areas and are of uncertain age relations to Tbs, Tr, and Ta. Trt and Tri in or near the map area have yielded Oligocene and Miocene isotopic dates respectively (isotopic date samples 4, 11, and 12, table 1; Silberman and others, 1975). Overlying Ta elsewhere in Churchill County has yielded Miocene isotopic dates (Willden and Speed, 1974).

Five possibly Quaternary sedimentary units are shown on the map. All except QTg and Qt have been mapped primarily from aerial photographs. Terrace gravel and sand (QTg) a distinctive, ≥940 m-thick unit that crops out only in low ridges flanking Fourmile Canyon in the northwestern portion of the map, is the only Quaternary unit containing measured bedding. In Fairview Valley east of the northern SSR geophysical studies show ≤5800 feet of Cenozoic alluvium and a well penetrated 980 feet of alluvium (Beal and others, 1964).

All Tertiary–pre-Tertiary contacts in the southern SSR are mapped as fault or intrusive igneous contacts. Data supporting the presence of intrusive igneous contacts are given in the explanation; the following section will describe and document fault contacts.

Structures

Cenozoic faults

Cenozoic high-angle faults and low-angle contacts interpreted to be faults crosscut Cenozoic and pre-Cenozoic rocks. Low-angle contacts mapped as faults are typically

TABLE 1. ISOTOPIC DATE SAMPLE LOCALITIES

Locality on map	Unit, location	Sample number	Technique, mineral, lab	Date (Ma)	Reference
1*	MzPzhc, n2a	82088-3	$^{40}Ar/^{39}Ar$ on hornblende, lab analyzed: L. Snee, USGS, Denver	85.47 ± 0.33	Satterfield, 1995
2*	Trqp, n6a	9292-1	U-Pb on zircon, lab analyzed: J.E. Wright, Rice University	237 ± 5***	Satterfield and Oldow, 1996
3*	MzPzcs, n6c	92989-2	$^{40}Ar/^{39}Ar$ on actinolite, lab analyzed: L. Snee, USGS, Denver	~77	Satterfield, 1995
4	Tr, NE-most Margin	H93-149	$^{40}Ar/^{39}Ar$ on 8 sanidine crystals, lab analyzed: New Mexico Geochronology Research Laboratory	31.03 ± 0.15†	C. Henry, written commun., 1999
5*	Kg, granodiorite Nevada Scheelite pluton	AD-4	K-Ar on biotite, Geochron Laboratories	89.9 ± 1.0**	Schilling, 1964
6*	Kg, granodiorite Nevada Scheelite pluton	AD-7	K-Ar on biotite, Geochron Laboratories	85.9 ± 3.5**	Schilling, 1964
7*	Kg, granite Sand Springs pluton	AD-1	K-Ar on biotite, Geochron Laboratories	81.7 ± 2.0**	Schilling, 1964
8*	Kg, aplite-pegmatite Sand Springs pluton	AD-6	K-Ar on biotite, Geochron Laboratories	67 ± 4**	Schilling, 1964
9*	Kg, granodiorite Sand Springs pluton	AD-3	K-Ar on biotite, Geochron Laboratories	78.0 ± 2.0**	Schilling, 1964
10*	Kg, northern Sand Springs Range	9392-3	U-Pb on zircon, lab analyzed: J.E. Wright, Rice University	Cretaceous, ≥80***	Satterfield and Oldow, 1996
11	Trt, southwestern Sand Springs R.	H00-58	$^{40}Ar/^{39}Ar$ on 15 sanidine crystals, New Mexico Geochronology Research Laboratory	24.93 ± 0.06†	C. Henry, written commun., 2001
12	Trt, southwestern Sand Springs R.	H00-57	$^{40}Ar/^{39}Ar$ on 12 sanidine crystals, New Mexico Geochronology Research Laboratory	28.74 ± 0.07†	C. Henry, written commun., 2001
13*	Kg, aplite-pegmatite Sand Springs pluton	AD-2	K-Ar on biotite, Geochron Laboratories	32.3 ± 3.0**‡	Schilling, 1964

*sample location on figure 1 **recalculated to present decay constants ***for additional data on this sample, see table 4 †data table at www.nbmg.unr.edu/argon/sandsprings.htm
‡biotite shows “considerable alteration to chlorite” and age is suspect (Wilden, 1964)

contacts between Trt and pre-Cenozoic map units. These contacts have also been interpreted to be an unconformity where tuffs were deposited on an irregular topographic surface on pre-Cenozoic rocks (C. Henry, written commun., 2002). Contacts between pre-Cenozoic rocks and Trt that appear to be low angle are interpreted to be faults because, where well exposed and easily measured, compaction foliation in Trt directly overlying contacts dips at steep angles, implying that the foliation was crosscut by underlying faults (relations shown on cross sections C–C', D–D', and E–E'). One such locality is near isotopic date sample locations 11 and 12, along the western margin of the range at the southern margin of n6c. There the well-located Trt–pre-Cenozoic contact follows contour lines for more than 1 km suggesting the contact is planar and low-angle. Given the assumption that the contact is planar, a three-point calculation indicates the contact dips 7°SW. Abundant measured compaction foliations in Trt adjacent to the contact and throughout this nearly 1 km^2 local area dip fairly consistently 24°–66° southwestward. In the same locality, Tru, a cooling unit subdivision within Trt, abruptly stops at the Cenozoic–pre-Cenozoic contact to the north, apparently because Tru is truncated by a fault. Low-angle faults in the northern Gillis Range, 20 km to the southwest, and in the Gabbs Valley Range, the southward continuation of the Gillis Range, are interpreted to be décollement surfaces at the base of transtensional nappes within the Walker Lane (Hardyman and Oldow, 1991).

An alternative interpretation must be considered. Basal Trt contacts locally or throughout the SSR could be unconformities atop irregular paleotopography since this contact type is common throughout western Nevada and the Sierra Nevada (Dilles and Gans, 1995). Direct indicators of low-angle fault movement, such as slickenlines on polished fault surfaces, have not been found on Cenozoic–pre-Cenozoic contacts in the SSR. Offset senses or amounts of displacement on interpreted low-angle faults in the SSR remain unknown. As expected at and above an unconformity at isotopic date sample location 12 the contact between pre-Cenozoic rocks and Cenozoic ash-flow tuff is marked by a conglomerate of well-rounded boulders of pre-Cenozoic rocks up to 50 cm in diameter. These are overlain progressively upward by bedded tuff, poorly exposed conglomerate(?) marked by a lag of rounded boulders, and poorly welded tuff that passes upward into a densely welded vitrophyre and then densely welded devitrified tuff (C. Henry, written commun., 2002). In addition, in some areas, such as in Trt east of Scheelite Summit, existing sparse data apparently show compaction foliation orientations are not consistent in strike or dip, relations expected if compaction occurred above irregular paleotopography.

High-angle faults that dissect the entire southern SSR offset Cenozoic map units, Cenozoic low-angle faults, and pre-Cenozoic map units and structures. In general they produce topographic saddles and range front scarps, prominent at the western boundary of n6a and along the eastern range front at the Sand Springs pluton-Quaternary contact. Locally they are identified as several-meter-thick zones of fault breccia, as slickenside surfaces, and as zones of quartz veins and/or jasper mineralization commonly explored by prospect pits and shafts. High-angle faults strike northwest and northeast to north-northeast. Several prominent faults in the southern SSR, such as the fault separating n7a-c from n6b-d, have arcuate traces that vary from east-west to north-northeast over ≤5 km distances. Slickenside surfaces along western range front faults dip westward 67° to 80° and contain lineations indicating dip-slip and strike-slip displacements. Mineralized zones along northwest-striking high-angle faults along the western range front have been explored in at least two mines (table 2) and in many prospect pits. Northwest striking high-angle faults along the western range front fall within and are probably parts of the easternmost Walker Lane (Hardyman and Oldow, 1991; Dilles and Gans, 1995).

Cenozoic faults do not reorient significantly Mesozoic structures or internally deform pre-Cenozoic rocks outside of their narrow fault zones. Mapped contacts show offsets on Cenozoic high-angle faults dissecting individual Mesozoic fault blocks are relatively small. Mesozoic contacts interpreted to be originally subhorizontal, D_2 thrust faults in the southern and northern SSR and an unconformity in the northern SSR (fig. 1; Oldow and others, 1993; Satterfield, 1995), remain subhorizontal. In addition the orientations of the two youngest generations of folds (D_2 and D_3), whose axial planes are nearly orthogonal, also remain consistent throughout the entire SSR (Satterfield, 1995) and have the same orientations as correlative phases in untilted domains elsewhere in western Nevada (e.g. Oldow, 1981, 1984).

Timing

Contacts mapped as low-angle faults crosscut 24.9 Ma Trt and are offset by high-angle faults. Cenozoic high-angle range front faults crosscut Quaternary alluvial fans (Qf) and are crosscut by active stream channels (Qa). In the northwest corner of the map, strata in Cenozoic terrace gravel and sand (QTg), are tilted eastward 40–60° in the footwall of west-dipping range front faults, suggesting range front faults moved after QTg deposition.

PRE-CENOZOIC GEOLOGY

Rock types

Pre-Cenozoic rocks are subdivided into 29 map units. They include the Sand Springs pluton, a Cretaceous granitoid batholith, smaller Cretaceous granitoid plutons to the south and southeast, and large exposures of Mesozoic metamorphic tectonites that flank the Sand Springs pluton.

Pre-Cenozoic tectonites

Tectonites are metamorphic rocks typically penetratively deformed during D_1 whose original compositions, bedding, and sedimentary structures remain recognizable to widely varying degrees. Pre-metamorphic rock types of tectonites

TABLE 2. MINES IN THE SOUTHERN SAND SPRINGS RANGE

Mine	Ore	Geologic setting, location	Production history	Reference
Crystal Claims	scheelite	Kg-JTrfp contact 2 miles ENE of Nevada Scheelite Mine	1939–1956 (intermittent): 280 units WO_3	Stager and Tingley (1988)
Eagleville or Eagle Mine	gold, tungsten	2 NW-trending quartz veins bearing gold and barite; 1 m, 6–9 m thick near JTrfp-MzPzf contact at Eagleville in SE portion of map	Gold discovered 1882: produced $50,000; 1954: 8 units WO_3	Ross (1961), Stager and Tingley (1988)
Nevada Scheelite	scheelite	0.5–15 m thick skarn at Kg-MzPzc contact; west flank Nevada Scheelite pluton; ore mined at 6 levels, deepest 500-foot depth	1935–1982 (intermittent): 315,000 units WO_3 includes several adjacent mines	Stager and Tingley (1988)
Unnamed prospects, western range front	traces gold, silver, copper	Ore in carbonate (MzPzc) and silicified tuff-breccia (Tr); at western rangefront ~1 mile N of county line. Felsite dikes (Tri?) crosscut MzPzc	Unknown: Prospect pits, 2 adits, 1 vertical shaft (Willden and Speed, 1974)	Willden and Speed (1974)
Rawhide Au-Ag Deposit	gold, silver	Mineralization in Miocene Rawhide volcanic center along NW-trending fault zone; ore concentrated in fractured andesite along hanging wall of rhyolite intrusion; gold also in quartz veins and lodes. Center of Rawhide mining area 4 km W of Nevada Scheelite Mine, outside map area	1907–1920, 1990–present; 1991 reserves: 29.4 million tons ore at 0.015 oz Au/ton and 0.23 oz Ag/ton	Black and others (1991), Ross (1961)
Rawhide Tungsten Deposit	scheelite	Skarn occurs at contact of carbonate (MzPzc?) and meta-andesite (JTrfp?) near Kg stock to NE, mineralization probably related to shears, fractures in carbonate. Dikes of Kg crosscut meta-andesite. Location uncertain, ~2 miles NW of Nevada Scheelite Mine or due N of Nevada Scheelite Mine	1950–1956: 382 units WO_3	Stager and Tingley (1988)
Red Ant Mine	scheelite	Skarn at Kg-MzPzac contact at bottom of 60-foot shaft at southern margin of Sand Springs pluton (see figure 1 for location)	1941–1980 (intermittent): 2650 units WO_3	Stager and Tingley (1988)
Sunnyside (Great Eastern) Mine	gold, silver	Free gold, horn silver, argentite, chrysocolla, and malachite in quartz at or near Kg-JTrfp contact, east flank of Nevada Scheelite pluton; exact location uncertain	Discovered 1874; occasional shipments in 1930s	Ross (1961)
Thorne Mine	scheelite	Kg-JTrfp contact, east flank of Nevada Scheelite Mine, 1 mile SE of Nevada Scheelite Mine, same general area as Sunnyside Mine	1974–1978 (intermittent): 339 units WO_3	Stager and Tingley (1988)

are diverse: mafic-intermediate volcanic/volcanogenic rocks and carbonate rocks comprise 48% and 30%, respectively, of the total exposed sections of tectonites (excluding intrusive igneous rocks), felsic volcanic and volcanogenic rocks comprises ~13%, and black shale comprise ~10% (fig. 3). Tectonites also include numerous intrusions of diverse, mafic and felsic compositions.

Although pre-metamorphic rock types of tectonites are generally recognizable, several factors prevent the assembly of a single continuous composite stratigraphic section for the southern SSR. First, tectonite rock types are heterogeneously distributed within 19 Mesozoic fault blocks (figs. 2, 3). Second, original stratigraphic unit thicknesses and facing directions remain unknown in most fault blocks due to deformation and metamorphism. Third, few fossils are preserved, so that ages of most map units are poorly constrained. Fourth, transitions between map units present few compelling lithologic correlations between sections in different fault blocks. Thus, figure 3 shows the stratigraphic successions of each Mesozoic fault block listed separately. The same succession of map units in different fault blocks, as in n6d and n7c (fig. 3), implies that in several cases correlations between fault blocks can be made.

Carbonate rocks in two map units in different Mesozoic fault blocks contain age-diagnostic fossils. A marble and felsic volcanogenic succession in n6a has yielded a single ammonoid characteristic of the late Early Norian (table 3). Probable megalodontid bivalve shell fragments characteristic of the Late Triassic are locally abundant in carbonate beds interstratified with felsic tuff at two localities in n6d (table 3). Other tectonite map units not in depositional contact with dated units, or not correlated to map units containing age-diagnostic fossils, are constrained to be Mesozoic and/or Paleozoic in age, since their original rock types predate D_1 metamorphism and deformation of Mesozoic age (documentation of D_1 timing in next section).

A preliminary date of the pre-D_1 quartz-feldspar porphyry intrusion (Trqp) is 237 ± 5 Ma (U-Pb on zircon, isotopic date sample 2, table 1; fig. 4), Middle Triassic in age (Geological Society of America, 1999). However well-exposed Trqp intrudes Trc which contains a Late Triassic ammonite. Several hypotheses can explain these contradictory relations. One possibility is that Trc varies in age, such that its base is Middle Triassic or older and its top is Late Triassic. Correlative limestone successions in the northern Gillis Range were deposited in deep marine environments where sedimentation rates are locally low (Oldow and others, 1993), allowing the possibility that the relatively thick Trc was deposited over a long interval of time. More biostratigraphic data in the SSR and in nearby areas can test this hypothesis. A second possibility is that Trc in n6a contains one or more additional, unmapped D_1 faults that juxtapose Trc containing the late Triassic ammonite against similar appearing, yet older carbonate rocks crosscut by Trqp. Pre- and/or syn-metamorphic D_1 faults are abundant in the southern SSR. Faults that juxtapose similar-appearing carbonate map units which typically lack preserved bedding would be very difficult to locate. A third possibility is that Trqp is Late Triassic and slightly younger than Late Triassic Trc. This would require that the absolute age picks for age boundaries shown in the Geological Society of America (1999) time scale are slightly inaccurate. This possibility merits consideration since estimated uncertainties of Middle and Late Triassic age boundaries are 8–9 million years and the isotopic date of Trqp includes a measurement uncertainty of ±5 million years. Trqp could be as young as 232 Ma (table 1) and the Carnian-Norian boundary could be as old as 230 Ma (Geological Society of America, 1999). Thus with current data, Trqp and Trc are allowably almost the same age. A slight revision of the isotopic date of Trqp or of the time scale could establish that Trqp is slightly younger than Trc.

Except for Trqp and Trfqp, tectonites that are intrusive igneous map units are constrained to be Jurassic and/or Triassic in age or Mesozoic and/or Paleozoic in age. Ages are constrained to be no older than the ages of the units they intrude.

TABLE 3. FOSSIL LOCALITIES

Locality on map	Unit, location	Sample number	Fossils identified	Age
1	Trc, n6a	71789-1	*Indojuvavites* cf. *I. angulatus* (identified by N.J. Silberling, 1989)	Magnus Zone, late Early Norian (Silberling, 1984)
2	Tr(?)ct, n6d	82392-6f	possible megalodontid bivalves (identified by N.J. Silberling from photographs)	Late Triassic
3	Tr(?)ct, n6d	101291-1	possible megalodontid bivalves (identified from photographs by N.J. Silberling)	Late Triassic
4	MzPzc, n7d(?)	62589-1	large echinoderm fragments	not age-diagnostic

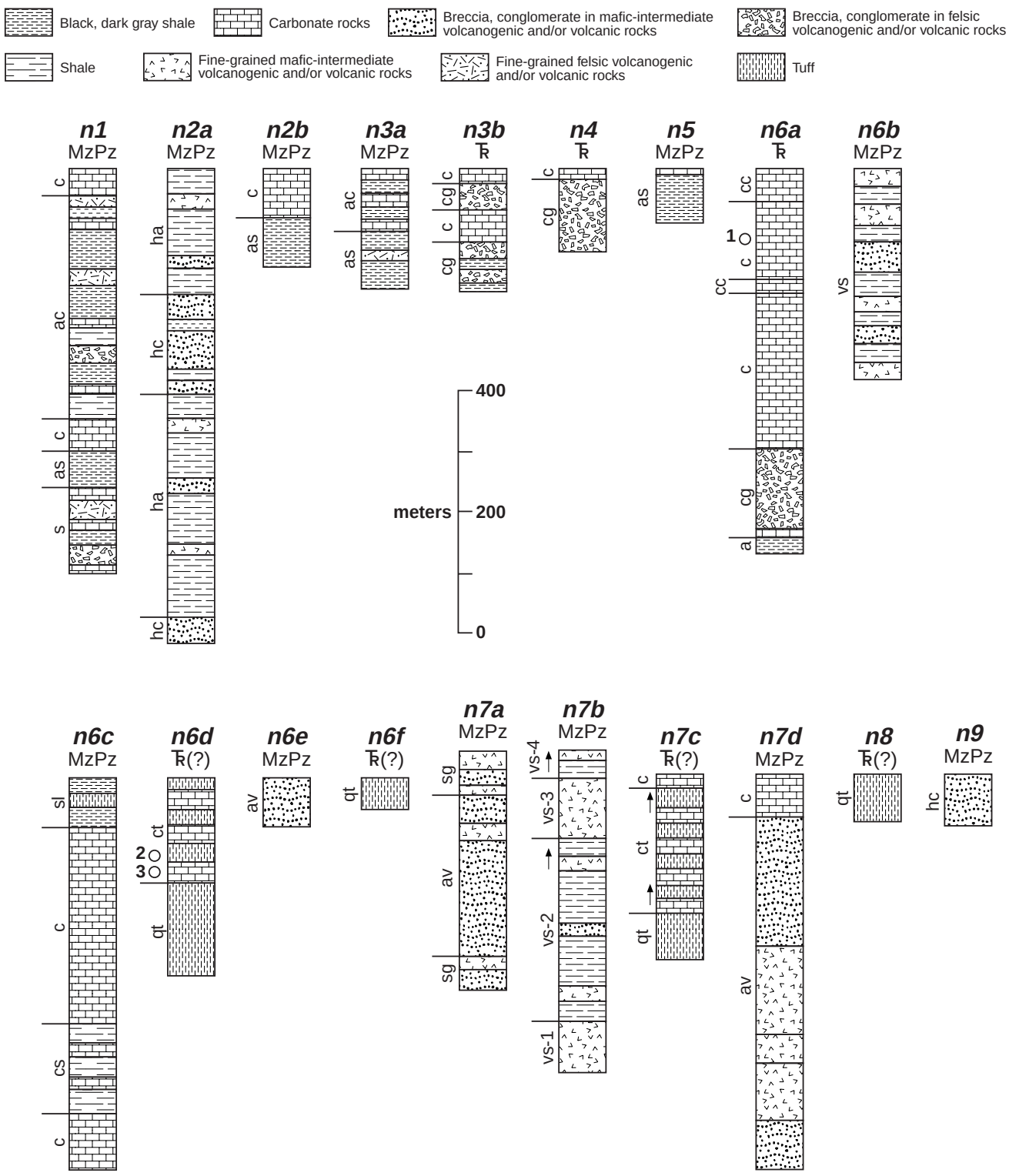

Figure 3. Stratigraphic columns of individual fault blocks in the southern SSR. Arrows to left of columns for n7b and n7c indicate where facing indicators have been found. Numbered circles indicate where age-diagnostic fossils have been found. Numbers are sample location numbers on map and in table 3. See plate for explanation of unit symbols.

Cretaceous granitoids

Cretaceous granitoid plutons scattered throughout the map area include: a) porphyritic granite apparently gradational to non-porphyritic granodiorite, b) aplite and pegmatite dikes and sills, and c) quartz veins. The most abundant rock type is coarsely crystalline porphyritic granite to non-porphyritic granodiorite mapped as Kg (mineral compositions in explanation). The Sand Springs pluton in the north, the largest pluton, is exposed over ~250 km^2.

Mapped and outcrop-scale granitoid plutons include large sills (such as the pluton crosscutting the n7c–n7d(?) boundary), plutons crudely disc-shaped in outcrop pattern (Nevada Scheelite pluton and pluton in southern n6b), and many smaller dikes and sills (several mapped adjacent to the Sand Springs pluton). The extensive southern intrusive contact of the Sand Springs pluton is overall parallel to S_1 in adjacent tectonites. However, at the scale of the map this contact is very irregular, locally crosscutting S_1 at high angles. Aplite and pegmatite dikes and sills centimeters to tens of meters thick are abundant near the Sand Springs pluton contact and crosscut granite and granodiorite throughout the Sand Springs pluton (Beal and others, 1964). Most aplite and pegmatite plutons have planar, steeply dipping contacts trending N50°W (Beal and others, 1964), including several mapped 0.5 km east of the Red Ant Mine. Locally, such as 3 km southeast of the Red Ant Mine, strikes of sill and dike contacts vary from north-south to east-west, dip angles vary 45–90°, and contacts display apparent pinch-and-swell features. However, varied dike orientations do not define folds, and variations in dike thickness do not define lineations (Satterfield, 1995). Felsic sills and plutons similar in composition to aplite and pegmatite plutons but not near granite contacts are mapped separately as CzMzi. Only larger plutons are mapped. At least one is apparently Cenozoic (see explanation) and unrelated to Cretaceous granitoid. Quartz veins are common near Kg contacts but are too thin to be mapped.

Granite and granodiorite comprising most of Kg is relatively homogeneous and boundaries between porphyritic granite and non-porphyritic granodiorite are indistinct. Rare compositional layering is a magmatic not a tectonic feature; near the Kg contact 0.5 km east of the Red Ant Mine steep north-south compositional layering (plotted on map) parallels the Kg contact and is orthogonal to S_1. Joints are a common internal feature in Cretaceous granitoid plutons; the most common set in the Sand Springs pluton strikes N50ºW, parallel to aplite and pegmatite dikes. A younger set of closely spaced fractures strikes N30ºE (Beal and others, 1964). Three joint orientations in two plutons are plotted on the map.

Granitoid intrusive contacts are in general well exposed and can be located within several meters. Fairly common hard-rock contacts are knife-sharp boundaries between typical, foliated metamorphic tectonite and coarsely crystalline, typical granitoid which sharply crosscuts well-preserved S_1 in tectonite. Contacts are steep and non-planar overall. The southern contact of the Sand Springs pluton, the most extensively exposed intrusive contact in the range, strikes northwest overall but at numerous places strikes north or even northeast. Extensive mine workings and exploratory drilling to over 500-foot depths along the west flank of the Nevada Scheelite pluton reveal its intrusive contact changes dip from sub-vertical to 30° and that portions of the northeast-striking contact dip northwest and southeast (Stager and Tingley, 1988).

Several mines, including the Nevada Scheelite Mine, have exploited thin, typically discontinuous zones of

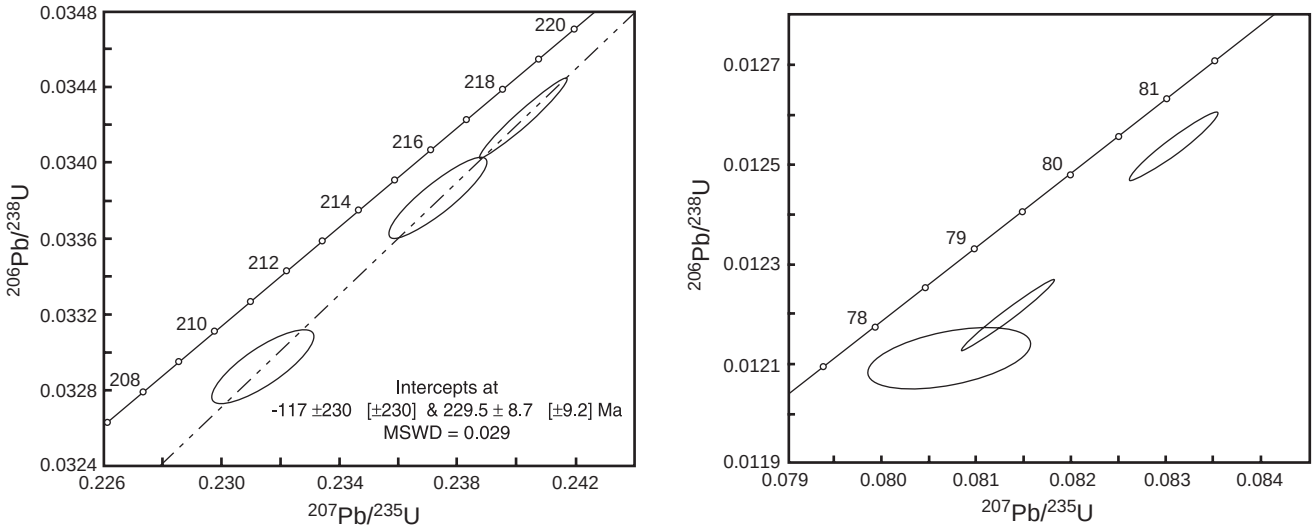

A) TRqp from sample locality 2 (located on geologic map) **B) Kg from sample locality 10 (located on fig. 1)**

Figure 4. Concordia diagrams of zircon size fractions from Triassic white-yellow quartz-feldspar porphyry pluton (A) and Cretaceous granitoid (B). Data-point error ellipses are 2σ.

scheelite mineralization at the Kg-country rock contact (Ross, 1961; Stager and Tingley, 1988, table 2). Ore minerals have been found at Kg-MzPzc and Kg-JTrfp contacts (table 2). Reported mineralized zones vary in thickness from 0.6 to 15 m (table 2). A twelve-kiloton nuclear bomb was detonated at the bottom of a 1,200-foot shaft within the Sand Springs pluton at the location of isotopic date samples 7 and 8 (fig. 1) on October 26, 1963 (Mackedon, 1990).

Mesozoic Structures

First-phase (D_1) Structures

D_1 folds and faults control the outcrop pattern of metamorphic tectonites in the northern and southern SSR. Outcrop-scale D_1 folds, foliation, and lineations are abundant in tectonites in the map area. Locally in the southern and northern SSR more than one phase of D_1 folds and fabric are recognized (Satterfield, 1995). Multiple D_1 phases are outcrop-scale features only and are not shown on the map.

D_1 folds. D_1 folds are tight to isoclinal flexures containing widespread penetrative axial-planar cleavage. Outcrop-scale D_1 folds of several millimeters to 0.5 m half-wavelength are defined by changes in bedding (S_0) and quartz vein orientation. They are common, yet irregularly distributed, in carbonate rocks, black slate/schist, and felsic and mafic volcanogenic and volcanic rocks. Outcrop-scale fold data are not plotted on the map (many data and descriptions of outcrop-scale folds are in Satterfield, 1995). Map-scale folds of 25 m to >1 km half-wavelength, many shown on the map by a thin line locating the surface trace of the axial plane, are defined in several ways. Many are identified by bends of depositional contacts crosscut by a consistent S_1 orientation. These relations are shown on the map in n1, 1 km east of the Red Ant Mine, in n7b on the northeast flank of Big Kasock Mountain, and in n6a, n7a, and n2a. D_1 folds are also sharp bends of the JTrfp-MzPzc contact, an intrusive igneous contact south of the Nevada Scheelite Mine that is crosscut by consistent S_1. Other D_1 folds are defined by changes in S_0 strike and/or facing direction crosscut by consistent S_1 orientation. These relations are shown in n7b within MzPzvs$_2$ on the north side of Scheelite Summit (cross section E–E'), in n7b northwest of Big Kasock Mountain, in southern n6b, in n7a, and in northwestern n6a. In addition, D_1 folds are mapped as bends in early-formed syn-D_1 faults, such as warps of faults separating n6a from n6b and n7a from n7b.

D1 folds are close to isoclinal and display rounded hinges. S_1, the foliation axial planar to map- and outcrop-scale folds, is typically a penetrative metamorphic foliation. Oriented chlorite, biotite, white mica, calcite, actinolite, hornblende, andalusite, and epidote define S_1. In MzPzas, Trqp, and Trfqp S_1 is also locally a penetrative, closely spaced fissility. In JTrfp S_1 is a sporadically developed spaced cleavage. S_1 orientations, the most abundant symbol on the map, are measurements at significant locations or a representative fraction of measurements collected.

S_0–S_1 intersection, mineral, and stretching lineations are geometrically related to D_1 fold axes and axial planes. S_0-S_1 intersection lineations, defined by the intersection of original bedding (S_0) and S_1, are parallel to map- and outcrop-scale D_1 fold axes (data in Satterfield, 1995). S_0–S_1 intersection lineations, not plotted on the map, can be constructed from abundant S_0 and S_1 data in n3a, n6a, n6b, n7b, n7c, and n7d. Stretching lineations, defined as long axes of elongate grains, pebbles, and cobbles of various compositions, plot within the S_1 plane (stereonets in Satterfield, 1995, in prep.). Stretched clast dimensions in the X-Z plane vary from 1.5:1 to 20:1. Stretching lineations are abundant within and representative measurements are plotted in n1, n2a, n3a, n3b, n6a, n6b, and n7b. D_1 mineral lineations, defined as long axes of syn-D_1 metamorphic minerals, form maxima parallel to stretching lineations (stereonets in Satterfield, 1995, in prep.). Long axes of actinolite, hornblende, andalusite, and aggregates of biotite crystals define mineral lineations. Mineral lineations are abundant within and representative measurements are plotted in n1 and n2a.

Present orientations of D_1 fold and fabric elements can be simply described with individual Mesozoic fault blocks, although orientations have been reoriented by several deformation phases. Nappes n1–n6 generally contain northwest-striking, steeply southwest-dipping S_1 and D_1 axial planes. S_1 strikes northwest overall; deflections formed during D_2. Within individual domains in n1–n6, S_1 planes contain subparallel concentrations of D_1 fold axes, S_0–S_1 intersections, stretching lineations, and mineral lineations which plunge moderately to the southwest or west-southwest (data in Satterfield, 1995, in prep.). Nappe n7 contains two concentrations of poles to S_1, one in the northwest quadrant and one in the southeast quadrant. Fold axes and S_0–S_1 intersections form girdle distributions within each S_1 orientation in n7. In n7b at Scheelite Summit stretching lineations define a maxima within S_1 which plunges moderately to the northwest. In all Mesozoic fault blocks except n6a, S_1 and S_0 are subparallel, another indication of tight to isoclinal D_1 folding. In n6a S_1 is at a high angle to S_0 within a broad hinge area of a map-scale fold.

D_1 faults. Syn-D_1 faults are distinguished from D_2 faults by their characteristic sharp, non-brittle, steeply dipping contacts, as well as by their pre-D_2 timing. Although they are difficult to recognize as faults at the outcrop-scale, map relations show they fulfill several criteria for faults: 1) D_1 faults locally truncate otherwise continuous map unit contacts on one or both sides, 2) adjacent S_0 within an individual map unit is locally at a high angle to the fault plane, implying the fault truncated original bedding, 3) D_1 faults locally truncate map-scale D_1 folds. Table 5 specifies where these relations occur. The D_1 fault separating n6b from n6c and n6d both crosscuts and is folded by map-scale D_1 folds, establishing that D_1 faults were active during D_1. D_2 folds reorient D_1 faults and D_2 faults crosscut D_1 faults, also supporting movement during D_1. Rarely exposed D_1

TABLE 4. U-Pb ISOTOPIC DATA

Sample number***	U (ppm)	$^{206}Pb^*$ (ppm)	Measured Ratios** $\frac{^{206}Pb}{^{204}Pb}$	$\frac{^{207}Pb}{^{206}Pb}$	$\frac{^{208}Pb}{^{206}Pb}$	Atomic Ratios $\frac{^{206}Pb^*}{^{238}U}$	$\frac{^{207}Pb^*}{^{235}U}$	$\frac{^{207}Pb^*}{^{206}Pb^*}$	Apparent Ages (Ma) $\frac{^{206}Pb^*}{^{238}U}$	$\frac{^{207}Pb^*}{^{235}U}$	$\frac{^{207}Pb^*}{^{206}Pb^*}$
SSR 9292-1, +150	1302	37.84	837	0.06842	0.15922	0.03382(17)	0.23737(133)	0.05091(13)	214.4 ± 1.1	216.3 ± 1.1	236.6 ± 5.9
SSR 9292-1, 150-210	1345	38.06	569	0.07673	0.18052	0.03294(16)	0.23156(143)	0.05099(18)	208.9 ± 1.0	211.5 ± 1.2	240.2 ± 8.4
SSR 9292-1, +210	1298	38.19	2116	0.05781	0.13042	0.03424(17)	0.24023(124)	0.05088(6)	217.0 ± 1.1	218.6 ± 1.0	235.5 ± 2.8
SSR 9392-3, +150	602	6.49	2390	0.05422	0.11775	0.01254(6)	0.08310(44)	0.04807(7)	80.3 ± 0.4	81.0 ± 0.4	102.6 ± 3.6
SSR 9392-3, 150-210	877	9.12	3754	0.05227	0.13507	0.01210(6)	0.08066(73)	0.04835(37)	77.5 ± 0.4	78.8 ± 0.7	116.3 ± 17.8
SSR 9392-3, 210-235	715	7.48	3658	0.05237	0.12160	0.01219(6)	0.08128(42)	0.04835(5)	78.1 ± 0.4	79.3 ± 0.4	116.4 ± 2.5

*Radiogenic Pb, corrected for common Pb **Isotopic compositions corrected for mass fractionation ***+150, 150–210, +210, and 210–235 are mesh size fractions

TABLE 5. MAP RELATIONS SUPPORTING D_1 FAULT CONTACTS

D_1 fault at boundary of	Fault block	Evidence
n2a-n2b	n2b	fault truncates S_0 in MzPzas
n3a-n3b	n3b	fault crosscuts Trqp-Trc contact
	n3a	fault crosscuts MzPzas-MzPzac contact
n6a-n6b	n6a	fault crosscuts Trc-Trcg, Trcg-Tra, and Trqp contacts
	n6a	fault truncates S_0 in Tra
	n6b	fault truncates S_0 in MzPzvs
n6b-n6d	n6d	fault crosscuts 2 Tr(?)ct-Tr(?)qt contacts
	n6d	fault truncates 2 map-scale D_1 folds
n7a-n7b	n7a	fault crosscuts MzPzav-MzPzsg contact
	n7a	fault truncates S_0 in MzPzav
	n7b	fault truncates S_0 in $MzPzvs_2$
	n7b	fault crosscuts $MzPzvs_2$-$MzPzvs_3$ contact
n7b-n7c	n7b	fault truncates S_0 in $MzPzvs_2$ east of Big Kasock Mtn
	n7b	fault crosscuts $MzPzvs_3$-$MzPzvs_4$ contact
	n7b	fault crosscuts $MzPzvs_2$-$MzPzvs_3$ contact
	n7c	fault crosscuts Tr(?)ct-Tr(?)qt
n7b-n7d	n7b	fault crosscuts $MzPzvs_2$-$MzPzvs_3$ contact north of Scheelite Summit
	n7b	fault truncates S_0 in $MzPzvs_2$ north of Scheelite Summit
n7c-n7d	n7c	fault crosscuts Tr(?)qt-Tr(?)ct contact

faults are zones no thicker than several centimeters that do not contain gouge or brecciated rocks. Similar-style faults in the Last Chance Range, southeastern California are several millimeter-thick zones tightly folded by subsequent deformation (Corbett, 1990a, b). In n1–n6, D_1 faults generally strike northwest and dip steeply southwest, parallel to S_1. In n7 faults strike northeast and are subvertical. Post-D_1 structures have reoriented D_1 faults and their original orientation and kinematic significance are not known.

Timing. D_1 in the SSR ended no later than Early Cretaceous. Poorly constrained ages of units deformed by and postdating D_1 structures in the northern SSR suggest that D_1 was confined to the Early through Late Jurassic. Several lines of evidence indicate that D_1 predated intrusion of Late Cretaceous granitoids. First, granitoid intrusive contacts commonly crosscut S_1 at high angles. Although margins of the Sand Springs pluton roughly parallel S_1, its irregular map-scale contact sharply truncates S_1 at many locations, such as 2 km north of its southernmost contact and 1 km east of the Red Ant Mine. Margins of other Kg plutons also sharply crosscut S_1, such as the western margin of the Nevada Scheelite pluton and at the southern boundary of n6c along the western range front. Second, granitoid plutons, including thin sills and dikes, are typically nonfoliated, homogeneous intrusions not displaying D_1 folds or fabric. Abundant, thin Kg dikes and sills adjacent to D_1 folds 3 km southeast of the Red Ant Mine are not folded and do not have orientations related to D_1 folds or fabric (data in Satterfield, 1995, in prep.). Third, in the northern SSR a small, well-exposed granitoid tentatively dated as Cretaceous (isotopic date locality 10, tables 1, 4) crosscuts metamorphic tectonites deformed in D_1, an overlying angular unconformity, and Cretaceous-Jurassic porphyritic basalt extruded atop this unconformity which is not metamorphosed or deformed in D_1 (fig. 1). This relation establishes that granitoid emplacement occurred after a post-D_1 unconformity and after extrusion of Cretaceous-Jurassic basalt above that unconformity (small-scale map in Oldow and others (1993); Satterfield, 1995, in prep.). Fourth, emplacement of Kg will be shown in the next section to postdate D_2, during which D_1 structures and fabric were folded and faulted.

The ostensibly youngest map units in the SSR deformed during D_1 are Jurassic(?) carbonate and quartz-rich siliciclastic rocks only exposed in the northern SSR. These units contain quartz arenite lithologically correlative to the Jurassic Westgate Formation in the southernmost Clan Alpine Mountains, and to the Jurassic Dunlap Formation exposed in several mountain ranges to the south (Oldow and others, 1993; Satterfield, 1995, in prep.). The oldest unit in the SSR not deformed or metamorphosed in D_1 is Cretaceous-Jurassic porphyritic basalt exposed only in the northern SSR (fig. 1, Oldow and others, 1993). This basalt has been correlated to lithologically similar extrusive equivalents of the 159 Ma Humboldt lopolith (Willden and Speed, 1974; Hudson, 1988). If these speculative age constraints based on lithologic correlations hold, D_1 is limited to the Jurassic, between 200 and 159 Ma.

However syn-D_1 amphibole separates from two separate tectonite samples have yielded Late Cretaceous $^{40}Ar/^{39}Ar$ dates (isotopic date samples 1, 3; table 1; fig. 5), similar to dates of Cretaceous granitoid. In light of multiple lines of field evidence suggesting Cretaceous granitoids were emplaced after D_1 and after D_2, Late Cretaceous isotopic dates from syn-D_1 minerals are interpreted to date when isotopic ratios where reset by heat from nearby post-tectonic granitoid emplacement. Temperatures of 500–550°C are required to reset hornblende isotopic ratios (Harrison, 1981). Although Cretaceous plutons are widespread throughout the SSR and isotopic date sample 1 is located only 0.2 km from the Kg contact, no obvious petrographic or $^{40}Ar/^{39}Ar$ data signature in isotopic date samples indicates that dates were reset.

Second-phase (D_2) structures

Mapped and inferred D_2 faults bound nappes n1–n9. Map- and outcrop-scale D_2 folds are abundant and well exposed throughout the map area. D_2 structures are directly superposed at the outcrop- and map-scale on D_1 folds, faults, and fabric.

D_2 folds. D_2 folds are typically close folds of S_1 which lack axial-planar cleavage. Outcrop-scale folds of 5 to 100 cm half-wavelength are defined by changes in orientations of S_1 and S_0 and are most abundant in carbonate rocks and black slate/schist. Outcrop-scale fold data are not plotted on the map; outcrop-scale fold data are in Satterfield (1995, in prep.). Map-scale folds of 0.2 to 5 km half-wavelength, many identified on the map by positions of the surface trace of axial planes, are defined several ways. First, D_2 folds are warps of depositional and intrusive contacts of metamorphic tectonites. Such warps include atypical "fish-hook" folds in n1 and n3b east and south of the Red Ant Mine which display greatly attenuated short limbs resulting from folding of three map units of differing competence (Ramsay and Huber, 1987). Second, numerous D_2 folds are defined by dramatic bends in S_1 form surfaces. Many such folds are identified in the northwest portion of the map. The axial trace of the longest wavelength D_2 fold mapped (~5 km half-wavelength) is shown southwest of the southernmost tip of the Sand Springs pluton. This single, subvertically plunging fold covers the entire southern half of n6. Third, D_2 folds include warps of map-scale D_1 folds particularly well displayed 1 km southeast of the Red Ant Mine. Fourth, D_2 folds in n7, where D_2 fold axes are subhorizontal, are primarily defined by reversals in S_1 dip directions.

D_2 folds are gentle to close flexures containing rounded and angular hinges. D_2 folds overall trend northeast; orientations vary in different nappes. Nappes n1–n6 contain north-northeast striking, subvertical axial planes and steeply south-southwest plunging fold axes. Nappe n7 contains northeast to east-northeast striking, subvertical axial planes and subhorizontal to gently southeast- and northwest-plunging fold axes (stereonets in Satterfield, 1995, in prep.).

D_2 faults. Syn-D_2 faults are distinguished from D_1 faults by their characteristic brittle deformation style, their fairly unique low-angle orientation, as well as by their post-D_1 timing. D_2

faults truncate depositional and intrusive contacts, D_1 folds and faults, S_1, and at least one map-scale D_2 fold. Table 6 locates these map relations. Fault movement during D_2 is inferred from the fault at the base of n3 that shows mutually crosscutting relations with map-scale D_2 folds 2-3 km southeast of the Red Ant Mine. Similar mutually crosscutting relations between D_2 folds and D_2 faults are displayed in the northern SSR (Oldow and others, 1993; Satterfield, 1995, in prep.). Mutually crosscutting relations between a single fault and several folds result when a brief time of fault movement occurs within a longer interval of folding, such that the same fault crosscuts early D_2 folds and is later folded by late D_2 folds. Rarely exposed D_2 fault surfaces consist of a 1- to 2-m-thick zone of brecciated limestone and fine gouge best observed in the northern SSR (Oldow and others, 1993; Satterfield, 1995, in prep.). In the northwest portion of the map, where best exposed, D_2 faults are subhorizontal surfaces. Faults at the bases of n6 and n3 are particularly well exposed. Varied, subhorizontal to moderate dips of D_2 fault surfaces result in part from folding during D_2 and D_3. Although direct kinematic indicators have not been found, D_2 faults are interpreted to be thrust faults because they are correlative in relative timing and style to thrust faults documented in many parts of the Luning-Fencemaker thrust belt. Displacement on Luning-Fencemaker thrust faults occurred synchronously with formation of northeast-trending folds in numerous mountain ranges (e.g., Oldow, 1981, 1984). Northeast-trending Luning-Fencemaker folds are correlative in relative timing, style, and orientation to D_2 folds in the SSR (Satterfield, 1995, in prep.).

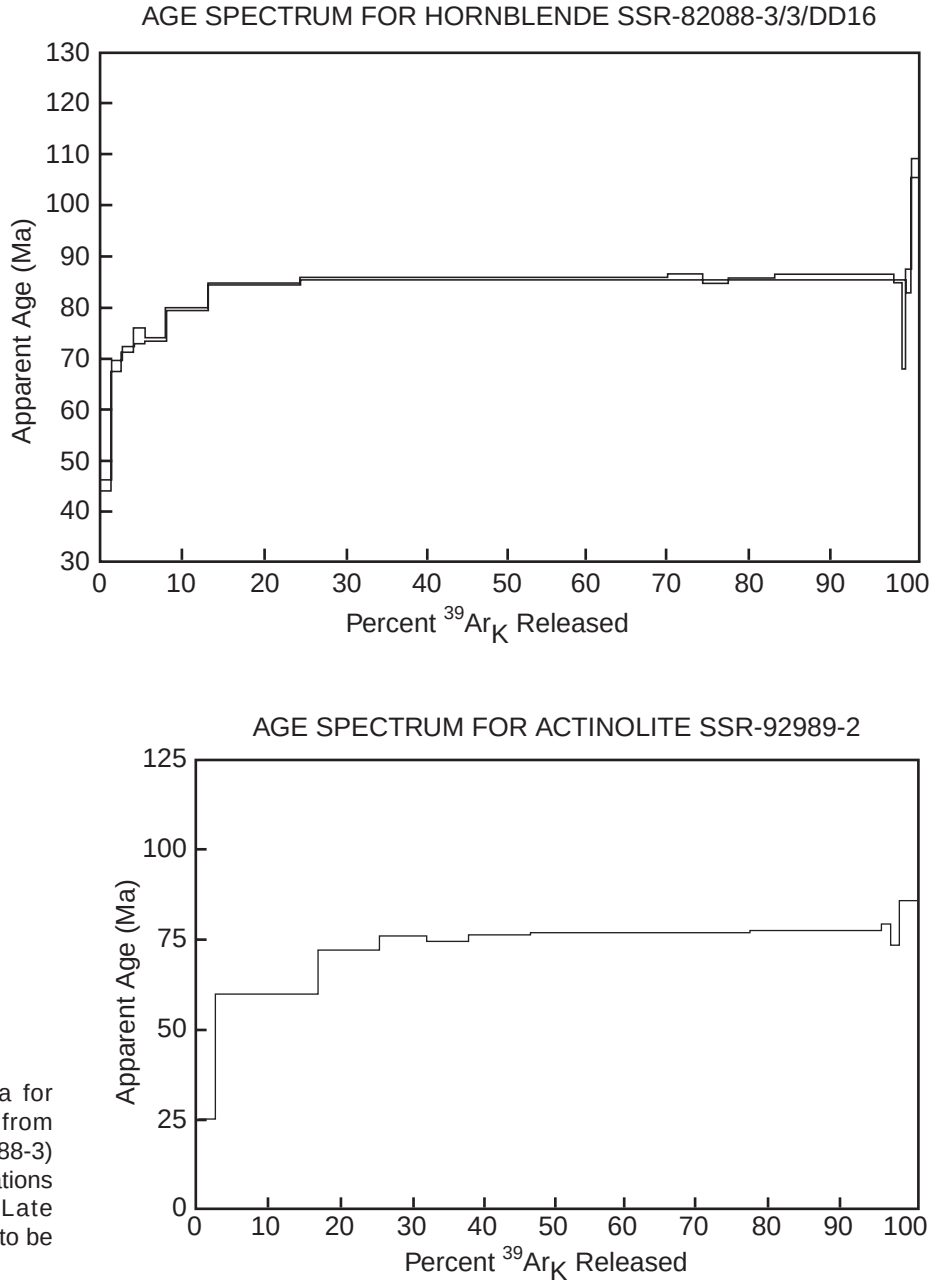

Figure 5. $^{40}Ar/^{39}Ar$ age spectra for tectonite amphibole separates from isotopic date samples 1 (SSR-82088-3) and 3 (SSR-9289-2). Sample locations are on the geologic map. Late Cretaceous dates are interpreted to be age of the Sand Springs pluton.

Some poorly exposed steep faults or portions of faults which crosscut D_1 folds could be: a) D_2 thrust faults steeply tilted by D_3 or late D_2 folds, or b) late-D_1 faults that retain their pre-D_2 steep orientation, or c) a combination of D_2 and D_1 faults. In these situations several alternative arrangements of different fault generations were considered and the simplest one shown on the map.

Timing. D_2 structures deform the youngest Mesozoic stratigraphic unit in the SSR, Cretaceous-Jurassic porphyritic basalt exposed only in the northern SSR. Late Cretaceous granitoids intruded after D_2. Several local observations in the southern SSR document this relative timing of Cretaceous plutons and D_2. First, the Sand Springs pluton crosscuts D_2 faults at the bases of n2 and n6b. Second, thin granitoid sills and dikes abundant near the Sand Springs pluton in n2a are not folded in outcrop-scale or map-scale D_2 folds. Three granitoid dikes mapped in n1 0.5 km east of the Red Ant Mine consistently trend northwest, crosscutting both limbs of a map-scale D_2 fold. Third, the extensive and well-exposed intrusive contacts of the Sand Springs pluton do not show evidence of extensive brittle shearing expected if this large pluton predated D_2 or D_3. Fourth, D_2 cleavage or syn-D_2 metamorphic minerals are not observed as Cretaceous plutons are approached, suggesting that D_2 is not related to their emplacement. The youngest map unit folded and crosscut by D_2 structures is the Cretaceous-Jurassic porphyritic basalt exposed in the northern SSR (Oldow and others, 1993; Satterfield, 1995, in prep.). Thus if speculative lithologic correlation to the dated Humboldt lopolith holds, D_2 is no older than 159 Ma. In summary, D_2 is inferred to have occurred before 85 Ma and possibly after 159 Ma.

Third-phase (D_3) Structures

The final phase of Mesozoic deformation, D_3, produced gentle to open folds lacking axial-planar cleavage that consistently strike northwest throughout the SSR. Relative timing of D_1, D_2, and D_3 is directly documented at location A in the southernmost SSR where D_3 folds are superposed on D_2 folds which in turn reoriented S_1 axial planar to outcrop-scale D_1 folds. D_3 folds are easily identifiable only in n7 and in the northern SSR because in these nappes many pre-D_3 surfaces were subhorizontal and thus readily folded into open flexures. D_3 folds are rarely recognized in n1 through n6, probably because S_0 and S_1 planes in these nappes were northwest-striking and steeply dipping, and thus more difficult to reorient by northeast-southwest compression. Outcrop-scale folds of 5 cm to 3 m half-wavelength are warps of S_0 and S_1 most abundant in carbonate rocks in the southern SSR (stereonets in Satterfield, 1995, in prep.). Map-scale folds of 40 to 400 m half-wavelength are defined by changes in orientation of S_0 and S_1; two are identified on the map in n7. D_3 axial planes strike on average N55°W, are subvertical, and contain fold axes steeply plunging to the northwest (Satterfield, 1995, in prep.). Strikes of axial planes vary from N10°W to N80°W.

D_3 folds, like D_2 structures, apparently formed between the mid-Jurassic and Late Cretaceous because in the northern SSR they fold the basal contact of Cretaceous-Jurassic porphyritic basalt (Satterfield, 1995, in prep.) and do not

TABLE 6. MAP RELATIONS SUPPORTING D_2 FAULT CONTACTS

D_2 fault at base of:	Fault block	Evidence
n2	n1	fault crosscuts MzPzc-MzPzac contacts
	n1	fault crosscuts MzPzas-MzPzs contacts
n3	n2a	fault crosscuts MzPzha-MzPzhc contacts
	n2a	fault truncates map-scale D_1 fold and S_1
	n2a	fault truncates map-scale D_2 fold
	n2a, n2b	fault crosscuts D_1 fault (n2a-n2b)
	n2b	fault truncates S_0 in MzPzas
	n3a	fault crosscuts MzPzas-MzPzac contact
	n3a	fault crosscuts D_1 fault (n3a-n3b)
	n3a	fault apparently truncates S_1
	n3a	fault truncates map-scale D_2 fold
n4	n3b	fault crosscuts Tkc-Tkcg contacts
	n3b	fault truncates map-scale D_1 fold
	n4	fault crosscuts Tkc-Tkcg contact
n6	n2a-n2b	fault crosscuts D_1 fault (n2a-n2b)
	n3b	fault crosscuts Tkc-Tkcg contact
	n3b	fault truncates map-scale D_1 fold
	n3b	fault truncates S_1
	n6a	Tkc highly fractured near fault
	n6a,n6b	fault crosscuts D_1 fault (n6a-n6b)

deform Late Cretaceous granitoids. Suggestions that granitoid emplacement postdated D_3 include the lack of brittle deformation along the margins of large plutons and the absence of D_3 folds in thin granitoid dikes.

KEY POINTS

The map, cross sections, and accompanying paper present a detailed picture of the geology of the southern Sand Springs Range. They illustrate four key points. First, the pre-Cenozoic section, although dismembered, is unusually thick and diverse in composition. It includes carbonate rocks, felsic tuff, mafic volcanogenic conglomerate, and black shale divided into 18 map units. Seven different pre-Cenozoic intrusive igneous map units, including metamorphosed felsic and mafic rocks and unmetamorphosed granitoid, crosscut Mesozoic and/or Paleozoic sections. This diversity in rock type is a primary, pre-metamorphic feature of Mesozoic and/or Paleozoic stratigraphy. Although tectonites are metamorphosed and deformed to varying degrees (Satterfield, 1995, in prep.), differences in protolith composition listed in the map unit descriptions and differences in successions of rock units within nappes preclude outwardly similar map units, such as green volcanogenic MzPzvs and MzPzhc, from being correlative. The total thickness of the pre-Cenozoic section exposed in the SSR may exceed 3–4 km, comparable in thickness to the thickest sections in other parts of the Mesozoic marine province (Oldow and others, 1993).

Second, the map area contains unusually well exposed and abundant map-scale and outcrop-scale folds separable into three generations: D_1, D_2, and D_3. Mesozoic rocks are typically penetratively deformed and metamorphosed by the first deformation phase, D_1, which includes folds, coeval faults, a pervasive axial planar foliation (S_1), stretching lineations, and mineral lineations. A second widespread deformation phase, D_2, produced abundant map-scale and outcrop-scale folds and faults, further shuffling the stratigraphy of the SSR. Several localities identified in this paper and/or symbolized on the map show D_2 folds directly superposed on D_1 folds and D_3 folds superposed on D_1 and D_2 folds. Orientations of folds and D_1 fabric plotted on the map also establish relative timing of D_1, D_2, and D_3. Several lines of evidence indicate that D_1 and D_2 predated intrusion of widespread Cretaceous granitoid plutons.

Third, the southern SSR provides a well-exposed view of the margins of the Sand Springs pluton and several smaller plutons. These Cretaceous granitoids sharply crosscut existing D_1–D_3 structures and metamorphic fabric and produced little deformation and metamorphism in their country rock. Surprisingly, $^{40}Ar/^{39}Ar$ dates of syn-D_1, pre-pluton emplacement amphiboles (isotopic date samples 1 and 3, table 1) are Cretaceous, overlapping ages of Cretaceous plutons. In light of several well-exposed field relations, isotopic clocks of syn-D_1 amphibole samples apparently have been reset by post-tectonic pluton emplacement long after the amphiboles originally crystallized.

Fourth, Cenozoic rocks and structures in the SSR are diverse and, except for the youngest Quaternary sedimentary units (Qa, Qt, Qf, and Qof), are interpreted to be everywhere in fault or intrusive contact with pre-Cenozoic rocks. The 13 Cenozoic map units distinguished include mafic and felsic intrusive and extrusive igneous rocks, sedimentary rocks, and sediments. Widespread Tertiary rhyolite (Tr) is an enigmatic map unit: it varies greatly in color and contains portions showing both intrusive and extrusive field relations. Cenozoic and older map units are also bounded by high-angle faults and by apparent low-angle contacts interpreted to be faults that separate Tertiary rhyolite, including tuff (Trt) from pre-Cenozoic rocks. Cenozoic terrace gravel (QTg) is the youngest map unit that has been steeply tilted by faulting. Range front faults unequivocally crosscut all Cenozoic units except modern stream channel deposits (Qa) and talus (Qt).

ACKNOWLEDGMENTS

John S. Oldow carefully reviewed several versions of this map in the field and in the office, leading to substantial improvements. Christopher D. Henry obtained isotopic dates of three samples in the field area, recalculated published K-Ar dates, and shared his knowledge of volcanic rocks. Norman J. Silberling identified fossils mentioned in the text. Bill McClelland generated concordia diagrams from U-Pb data. The map includes undergraduate research data of Caren Chaika, Edsel Townsend, Danny Do, Laurie Miller, and Tyler Barber. Field and laboratory work were supported by grants from the Arco Oil and Gas Company, the American Association of Petroleum Geologists, the Geological Society of America, Sigma Xi, Rice University, the Geological Society of Nevada, and National Science Foundation (grants to J.S. Oldow). Past and present owners of the Nevada Scheelite Mine, including NRD Inc., Tom C. Dyke, and John Spicer, provided access and shelter. Patrick J. and Jeanne McCartin, longtime caretakers at the Nevada Scheelite Mine, offered support in many ways.

REFERENCES

Banaszak, K.J., 1969, Geology of the southern Sand Springs Range, Mineral and Churchill Counties, Nevada [M.S. thesis]: Northwestern University, Evanston, Illinois, 35 p.

Beal, L.H., Jerome, S.E., Lutsey, I., Olson, R.H., and Schilling, J.H., 1964, Geology of the Sand Springs Range, *in* Nevada Bureau of Mines and Geology, Final report geological, geophysical, chemical, and hydrological investigations of the Sand Springs Range, Fairview Valley, and Fourmile Flat, Churchill County, Nevada, for Shoal Event, Project Shade, Vela Uniform Program, United States Atomic Energy Commission, p. 159–164.

Black, J.E., Mancuso, T.K., and Gant, J.L., 1991, Geology and mineralization at the Rawhide Au-Ag Deposit, Mineral County, Nevada, *in* Raines, G.L., Lisle, R.E., Schafer, R.W., and Wilkinson, W.H., eds., Geology and ore deposits of the Great Basin: Symposium proceedings: Geological Society of Nevada, p. 1123–1144.

Corbett, K.P., 1990a, Strain partitioning in thrust systems at mid-crustal depths: Characteristics of deformation in the Last Chance thrust system, east-central Nevada: Geological Society of America Abstracts with Programs, v. 22, p. 15.

Corbett, K.P., 1990b, Geologic map of the Last Chance Quadrangle, California and Nevada: U.S. Geological Survey Open-File Reports 90-0647-A and 90-0647-B, scale 1:62,500.

Dilles, J.H., and Gans, P.B., 1995, The chronology of Cenozoic volcanism and deformation in the Yerington area, western Basin and Range and Walker Lane: Geological Society of America Bulletin, v. 107, p. 474–486.

Ekren, E.B., and Byers, F.M., Jr., 1986, Geologic map of the Murphys Well, Pilot Cone, Copper Mountain, and Poinsettia Spring Quadrangles, Mineral County, Nevada: U.S. Geological Survey Miscellaneous Series Map I-1576, scale 1:48,000.

Geological Society of America, 1999, 1999 geologic time scale, 1 p.

Greene, R.C., Stewart, J.H., John, D.A., Hardyman, R.F., Silberling, N.J., and Sorensen, M.L., 1991, Geologic map of the Reno 1° by 2° Quadrangle, Nevada and California: U.S. Geological Survey Map MF-2154-A, scale 1:250,000.

Hardyman, R.F., and Oldow, J.S., 1991, Tertiary tectonic framework and Cenozoic history of the central Walker Lane, Nevada, *in* Raines, G.L., Lisle, R.E., Schafer, R.W., and Wilkinson, W.H., eds., Geology and ore deposits of the Great Basin: Symposium proceedings: Geological Society of Nevada, p. 279–301.

Harrison, T.M., 1981, Diffusion of ^{40}Ar in hornblende: Contributions to Mineralogy and Petrology, v. 78, p. 324–331.

Henry, C.D., 1996, Geologic map of the Bell Canyon Quadrangle, western Nevada: Nevada Bureau of Mines and Geology Field Studies Map 11, scale 1:24,000.

Hudson, M.R., 1988, Paleomagnetic and structural evidence bearing on the tectonic history of the Dixie Valley region, west-central Nevada [Ph.D. thesis]: Colorado School of Mines, Golden, 352 p.

John, D.A., 1992, Chemical analyses of granitic rocks in the Reno 1° by 2° Quadrangle and in the northern Pine Nut Mountains, west-central Nevada: U.S. Geological Survey Open-File Report 92-246, 35 p.

Mackedon M., 1990, Project Shoal: Anatomy of a nuclear event: Churchill County In Focus, v. 4, p. 11–22.

Oldow, J.S., 1981, Structure and stratigraphy of the Luning allochthon and the kinematics of allochthon emplacement, Pilot Mountains, west-central Nevada: Geological Society of America Bulletin, v. 92, part 1, p. 888–911.

Oldow, J.S., 1984, Evolution of a late Mesozoic back-arc fold and thrust belt, northwestern Great Basin, USA: Tectonophysics, v. 102, p. 245–274.

Oldow, J.S., Satterfield, J.I., and Silberling, N.J., 1993, Jurassic to Cretaceous transpressional deformation in the Mesozoic marine province of the northwestern Great Basin, *in* Lahren, M.M., Trexler, J.H., Jr., and Spinosa, C., eds., Crustal evolution of the Great Basin and Sierra Nevada: Cordilleran/Rocky Mountain Sections, Geological Society of America Guidebook: Department of Geological Sciences, University of Nevada, Reno, p. 129–166.

Proffett, J.M., Jr., and Proffett, B.H., 1976, Stratigraphy of the Tertiary ash-flow tuffs in the Yerington district, Nevada: Nevada Bureau of Mines and Geology Report 27, 28 p.

Ramsay, J.B., and Huber, M.H., 1987, The techniques of modern structural geology, volume 2: Folds and fractures: Academic Press, London, 700 p.

Ross, D.C., 1961, Geology and mineral deposits of Mineral County, Nevada: Nevada Bureau of Mines and Geology Bulletin 58, 98 p.

Satterfield, J.I., 1995, Mesozoic geology of the Sand Springs Range, west-central Nevada [Ph.D. thesis]: Rice University, Houston, Texas, 209 p.

Satterfield, J.I., and Oldow, J.S., 1996, Timing and significance of Jurassic-Cretaceous deformation phases in the Sand Springs Range, west-central Nevada: Geological Society of America Abstracts with Programs, v. 28, p. 108.

Schilling, J.H., 1964, Potassium-argon ages of the granitic intrusive rocks, *in* Nevada Bureau of Mines and Geology, Final report geological, geophysical, chemical, and hydrological investigations of the Sand Springs Range, Fairview Valley, and Fourmile Flat, Churchill County, Nevada, for Shoal Event, Project Shade, Vela Uniform Program, United States Atomic Energy Commission, p. 159–164.

Schweickert, R.A., and Lahren, M.M., 1990, Speculative reconstruction of the Mojave-Snow Lake fault: Implications for Paleozoic and Mesozoic orogenesis in the western United States: Tectonics, v. 9, p. 1609–1629.

Silberling, N.J., 1984, Map showing localities and correlation of age-diagnostic lower Mesozoic megafossils, Walker Lake 1° by 2° Quadrangle, Nevada and California: U.S. Geological Survey Miscellaneous Field Studies Map MF-2062, scale 1:250,000.

Silberman, M.L., Bonham, H.F., Jr., Garside, L.J., and Osborne, D.H., 1975, New K-Ar ages of volcanic and plutonic rocks and ore deposits in western Nevada: Isochron/West, no. 13, p. 13–21.

Speed, R.C., 1978, Paleogeographic and plate tectonic evolution of the early Mesozoic marine province of the western Great Basin, *in* Howell, D.G., and McDougall, K.A., eds, Mesozoic paleogeography of the western U.S.: Society of Economic Paleontologists and Mineralogists, Pacifc Section, Pacific Coast Paleogeography Symposium 2, p. 253–270.

Stager, H.K., and Tingley, J.V., 1988, Tungsten deposits of Nevada: Nevada Bureau of Mines and Geology Bulletin 105, 256 p.

Stewart, J.H., 1997, Triassic and Jurassic stratigraphy and paleogeography of west-central Nevada and eastern California: U.S. Geological Survey Open-File Report 97-495, 57 p.

Willden, R., and Speed, R.C., 1974, Geology and mineral deposits of Churchill County, Nevada: Nevada Bureau of Mines and Geology Bulletin 83, 95 p.

Wyld, S.J., Quinn, M.J., and Wright, J.E., 1996, Anomalous(?) Early Jurassic deformation in the western U.S. Cordillera: Geology, v. 24, p. 1037–1040.

Wyld, S.J., Rodgers, J.W., and Wright, J.E., 2001, Structural evolution within the Luning-Fencemaker fold-thrust belt, Nevada: progression from back-arc basin closure to intra-arc shortening: Journal of Structural Geology, v. 23, p. 1971–1995.

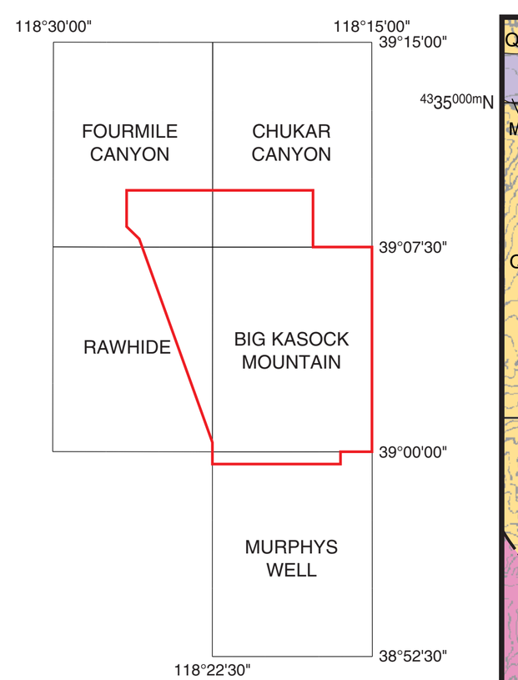

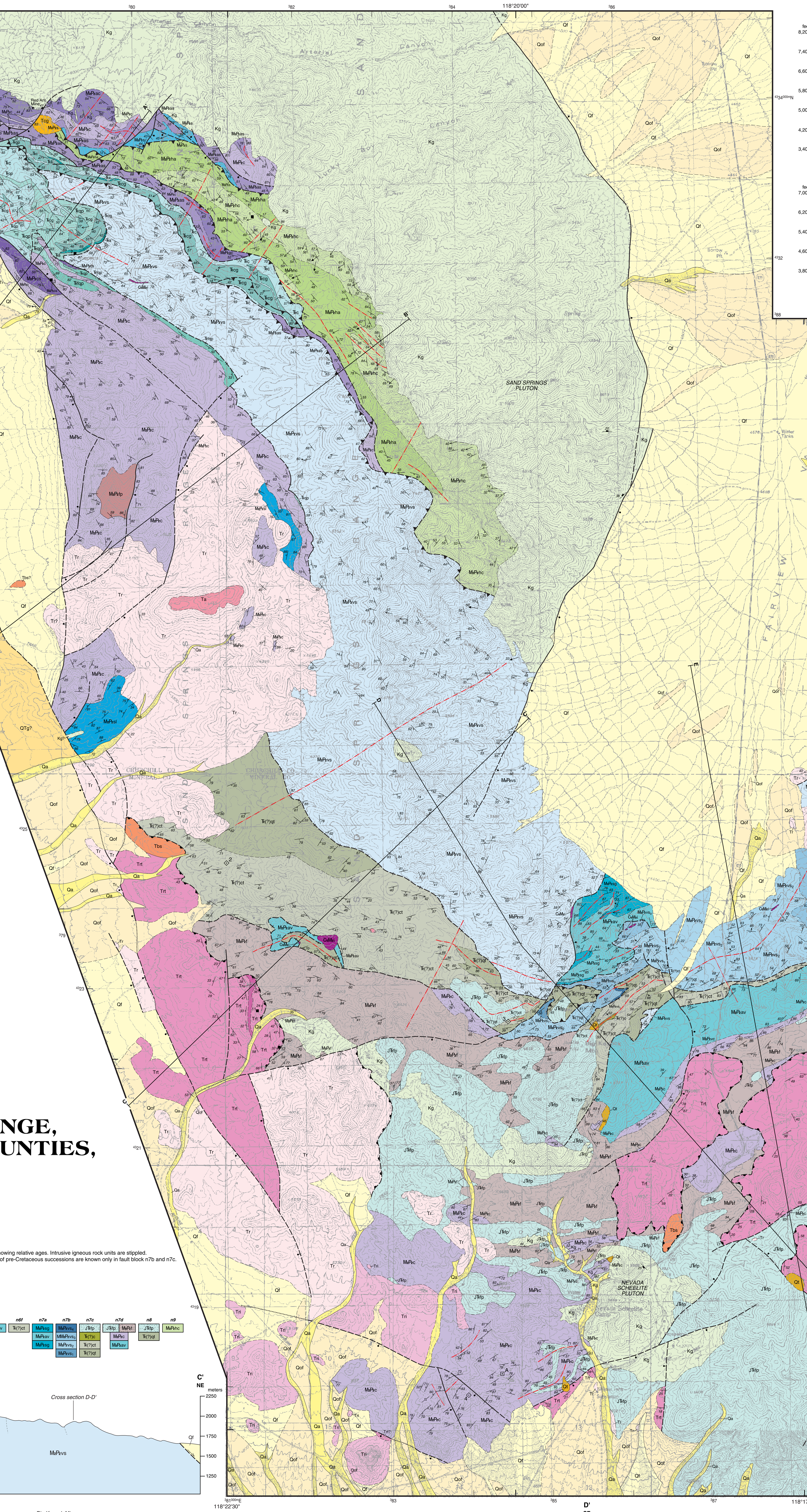

Scale 1:24,000

0 0.5 1 kilometer

0 0.5 1 mile

0 1000 2000 3000 4000 5000 feet

CONTOUR INTERVAL 40 FEET
SUPPLEMENTAL CONTOUR INTERVAL 20 FEET

Base map: U.S. Geological Survey
Big Kasock Mtn., Nevada 7.5' Quadrangle, 1980, Digital Raster Graphic (DRG);
Chukar Canyon, Nevada 7.5' Quadrangle, 1980, Digital Raster Graphic (DRG);
Fourmile Canyon, Nevada 7.5' Quadrangle, 1979, Digital Raster Graphic (DRG);
Murphys Well, Nevada 7.5' Quadrangle, 1980, Digital Raster Graphic (DRG);
and Rawhide, Nevada 7.5' Quadrangle, 1980, Digital Raster Graphic (DRG)

Depositional or intrusive contact Dashed where approximately located.

High-angle fault Dashed where approximately located; dotted where covered by Quaternary sediments; bar and ball on downthrown side; Cenozoic in age.

Low-angle fault Separating Cenozoic units from pre-Cenozoic units, scallops on upper plate; dashed where approximately located.

Low-angle fault Dashed where aproximately located; Mesozoic, syn-D_2 in age; teeth on upper plate; interpreted to be a thrust fault.

High-angle fault Dashed where approximately located; Mesozoic, syn-D_1 in age; offset sense unknown.

Surface trace of axial plane of D_1 fold.

Surface trace of axial plane of D_2 fold.

Surface trace of axial plane of D_3 fold Shown on map only in n7d.

Strike and dip of bedding (S_0).

Strike and dip of bedding (S_0), stratigraphic facing known to be upright.

Strike and dip of bedding (S_0), stratigraphic facing known to be overturned.

Strike and dip of compaction foliation in tuff within Tr.

Strike and dip of magmatic layering in Kg; only found near the Red Ant Mine in the northwestern portion of the map.

Strike and dip of metamorphic foliation and/or cleavage (S_1). Mesozoic, syn-D_1 in age.

Strike and dip of S_1 and bedding where S_1 and bedding are parallel.

Strike and dip of fault surface containing slickenlines and arrow indicating trend and plunge of slickenlines.

Strike and dip of joint surface in Kg.

Trend and plunge of stretching lineation defined by elongate clasts. Mesozoic, syn-D_1 in age.

Trend and plunge of mineral lineation. Mesozoic, syn-D_1 in age.

Location of age-diagnostic and significant fossils; descriptions of fossils summarized in table 3.

Location of sample providing isotopic date; descriptions and dates summarized in table 1.

Location of exposure in southernmost Sand Springs Range containing outcrop-scale, superposed D_1, D_2, and D_3 folds.

Original bedding (S_0); symbol only used on cross-sections.

Stratigraphic up direction interpreted from sedimentary structures; symbol only used on cross-sections.

Figure 2. Locations of Mesozoic fault blocks n1 through n9. Symbols used: CC, Chukar Canyon Quadrangle; BKM, Big Kasock Mountain Quadrangle; FC, Fourmile Canyon Quadrangle; R, Rawhide Quadrangle.

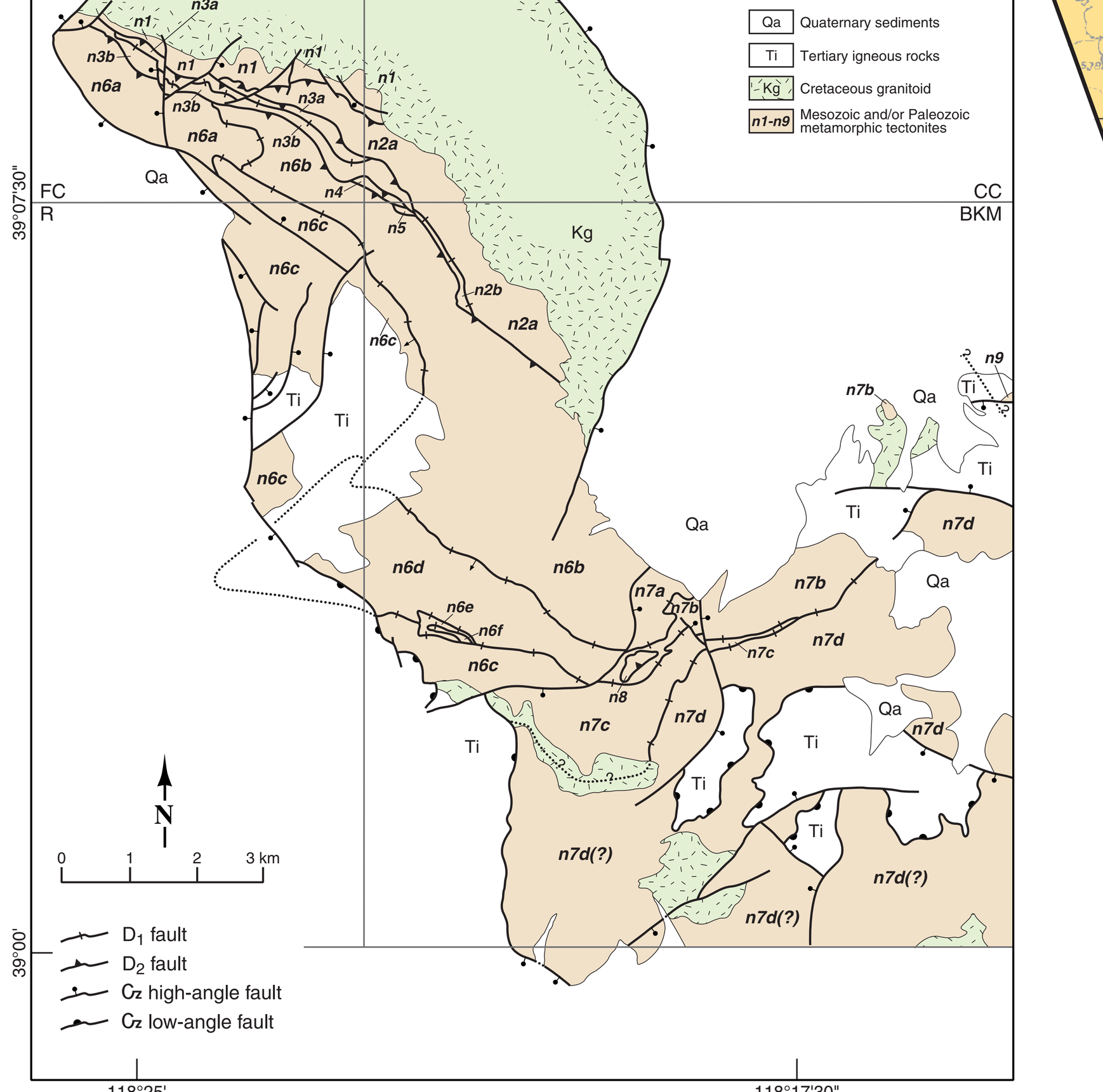

GEOLOGIC MAP OF THE SOUTHERN SAND SPRINGS RANGE, CHURCHILL AND MINERAL COUNTIES, NEVADA

Joseph I. Satterfield

2002

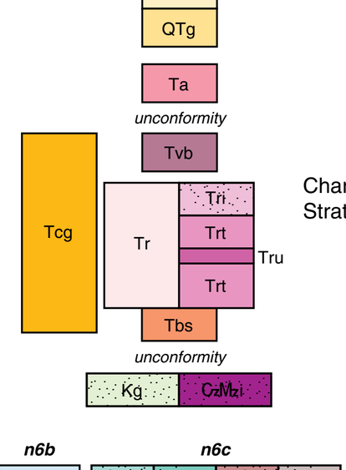

Chart of map units showing relative ages. Intrusive igneous rock units are stippled. Stratigraphic facings of pre-Cretaceous successions are known only in fault block n7b and n7c.

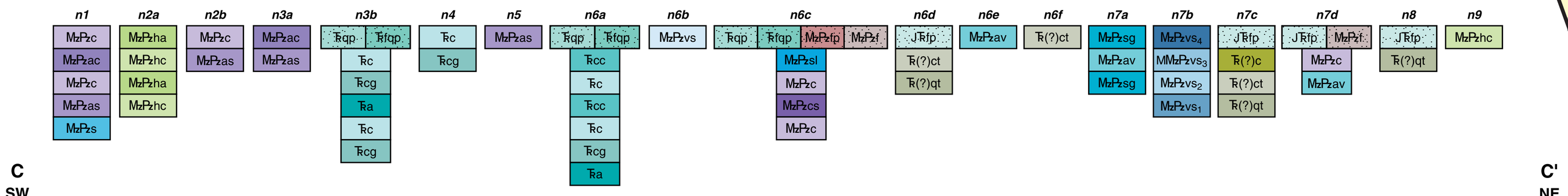

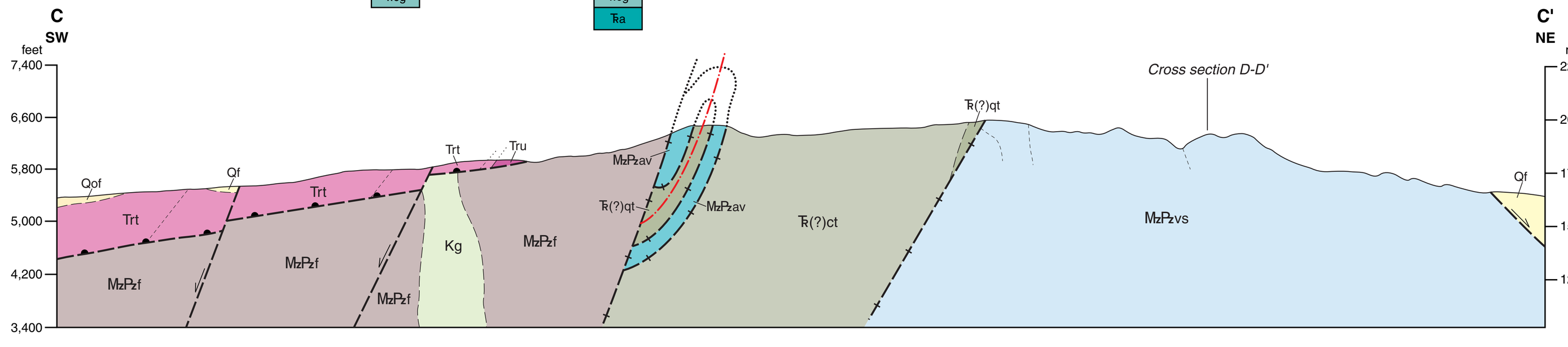

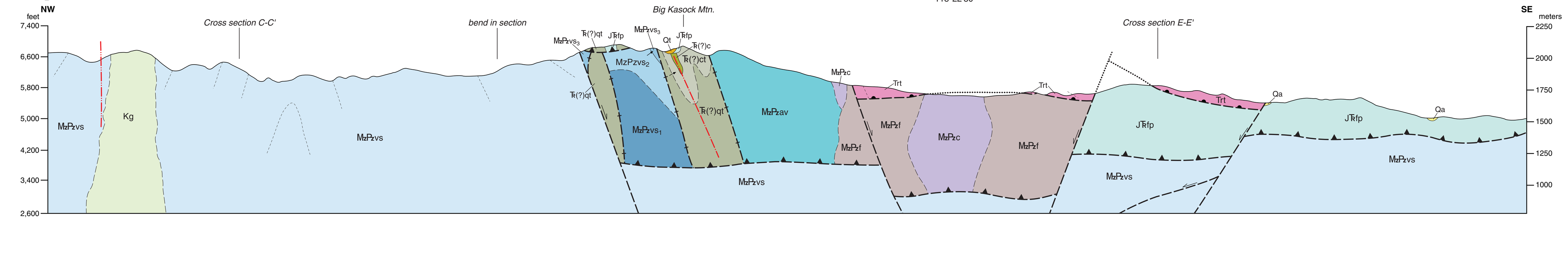

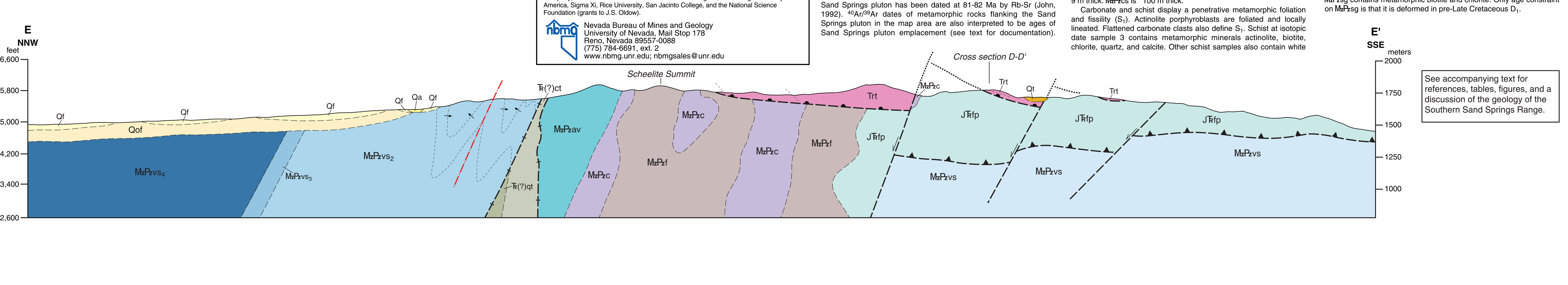

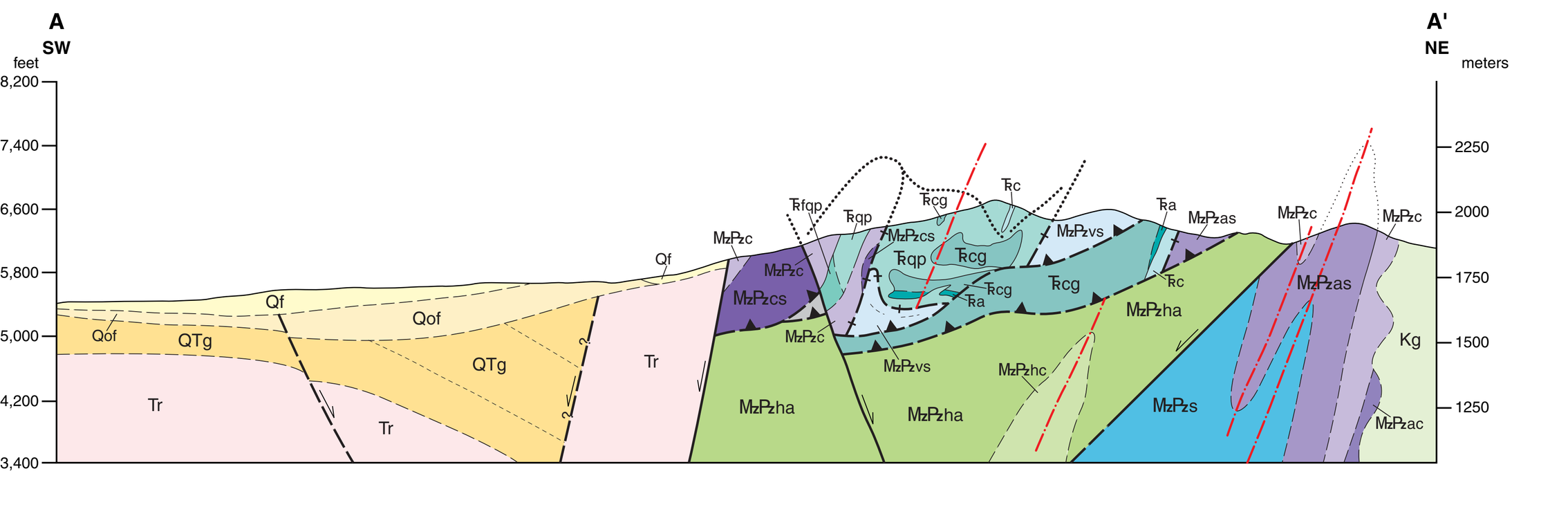

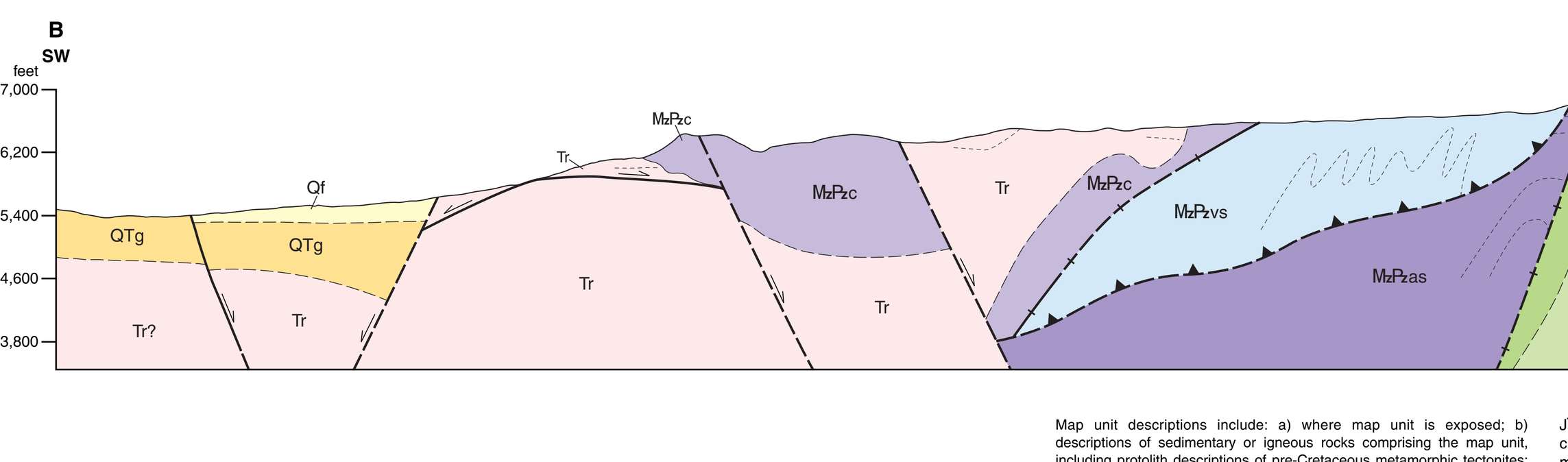

Map unit descriptions include: a) where map unit is exposed; b) descriptions of sedimentary or igneous rocks comprising the map unit, including protolith descriptions of pre-Cretaceous metamorphic tectonites; c) structural fabric and metamorphic mineral descriptions of metamorphic tectonite map units; d) age and age constraints; and e) how the unit can be distinguished from similar map units, if any. Locations of pre-Cretaceous map units are given in terms of Mesozoic fault blocks, labeled n1 through n9, that they are found within. The accompanying paper describes how fault blocks are delineated. Figure 2 (on this plate) shows the location of each fault block. A stratigraphic chart below figure 2 identifies map units in each fault block. Sedimentary or igneous rock descriptions cover minerals present, their crystal sizes, clast types and sizes, primary sedimentary or igneous structures, bed thicknesses, and overall map unit thicknesses. Map unit thicknesses are measured from cross sections and could differ greatly from pre-metamorphic thicknesses. Stratigraphic facings of pre-Cretaceous sections are generally not known. Sedimentary structures allow facings of successions in n7b and n7c to be determined. Descriptions of igneous rocks include evidence of intrusive or extrusive origin. Metamorphic minerals listed, unless noted otherwise, define a metamorphic foliation, S_1, that developed during the first deformation phase, D_1. The structural history of the range includes three phases of Mesozoic deformation, D_1 - D_3, described in the accompanying text.

Qa — Recent alluvium (Quaternary) Unconsolidated gravel, sand, and mud in active stream channels which crosscut all other map units. Unit identified by examining aerial photographs.

Qt — Talus (Quaternary) Unconsolidated gravel and sand in talus deposits on steep slopes.

Qf — Recent alluvial fan deposits (Quaternary) Unconsolidated sand, gravel, and mud in continuous fan or apron shapes. Upper surfaces typically have a smooth, undissected appearance on aerial photographs, although Qf includes several continuous fan shapes that are deeply dissected. Unit identified by examining aerial photographs.

Qof — Older alluvial fan deposits (Quaternary?) Unconsolidated sand, gravel, and mud in discontinuous exposures dissected by many small streams. Qf crosscuts this unit. Identified from aerial photographs.

QTg — Terrace gravel (Quaternary and/or Tertiary) Unconsolidated to slightly lithified tan sand and varicolored gravel only exposed in significant thickness in Fourmile Canyon and adjacent hills in northwest portion of map area. Angular and rounded gravel clasts up to boulder size include fragments of MzPzas, TRqp, Kg, and Tbs. Sandstone grains are dominantly 0.1-0.5 mm rounded quartz. Bedding is locally defined by contacts between lithified sandstone and conglomerate and by 1-2 mm laminations in sandstone. Maximum thickness is 460 m.

QTg is not metamorphosed or internally deformed. Cenozoic age of QTg is inferred from inclusions of Tertiary and Cretaceous units within, partly unconsolidated nature, and high stratigraphic and topographic position (overlies Tbs). Similar in description to the Tertiary gravel map unit in Bell Canyon Quadrangle, adjacent to the northeast, which is late Miocene to Pliocene (Henry, 1996).

Tcg — Cobble conglomerate (Tertiary?) Well-cemented gray-green conglomerate containing clasts of diverse composition exposed only in small exposures in Fourmile Canyon and near the Red Ant Mine in the northwest portion of the map. Mostly rounded clasts comprising 60% of rock range from 0.5 cm to 1.5 m long; averaging ~25 cm long. Clast types include granite, stretched pebble conglomerate, and feldpar porphyries differing in feldspar percent and matrix color. Matrix consists of 40-70% 1-3 mm feldspar grains or crystals and 1% quartz grains in a dark green matrix. No stratification recognized within.

Tcg is not metamorphosed or internally deformed. Probably Tertiary in age because unit contains probable Cretaceous granite inclusions, is not metamorphosed or internally deformed, and is more lithified than Quaternary units.

Ta — Porphyritic andesite (Miocene?) Medium-brown-weathering dark gray feldspar-hornblende porphyry exposed atop one ridge in the west-central Sand Springs Range (SSR). Porphyry consists of 1 mm feldspar and 3-10 mm hornblende crystals in an aphanitic matrix. No layering identified within. Ta is 34 m thick.

Unit is not metamorphosed. Ta is Tertiary or possibly Quaternary in age because horizontal lower contact overlies Tr. Correlative unit dated at 12.2 Ma and 17.6 Ma elsewhere in Churchill County (Willden and Speed, 1974).

Tvb — Flow breccia (Tertiary) Brown- and yellow-brown-weathering igneous breccia only exposed in western flank of Fourmile Canyon in the northwest portion of the map. Slightly rounded clasts 1-25 cm in diameter consist of 30-40% 1-2 mm feldspar laths in a medium gray aphanitic matrix. The matrix of breccia contains 50% phenocrysts in an aphanitic matrix. Phenocrysts in the matrix include 0.5-1 mm feldspar laths, 2-6 mm amphibole crystals, and sparse 0.5-1 mm quartz crystals. Clasts are sporadically distributed, comprising from 0-60% of the rock. No stratification identified. Tvb is not metamorphosed or internally deformed and appears to overlie Trt. Relative age relations between Tvb and Tri are unclear.

Tr (Tri, Trt, Tru) — Rhyolite intrusive rocks and crystal-lithic tuff (Oligocene and Miocene) White-, yellow-brown-, and reddish-brown-weathering quartz-feldspar-biotite porphyry and white to light-gray to maroon to glassy dark-brown crystal-lithic tuff extensively exposed on the western, southern, and eastern flanks of the range. Outcrop belts composed exclusively of intrusive quartz-feldspar-biotite porphyry are mapped as **Tri**. Outcrop belts composed of all crystal-lithic tuff are designated **Trt**. In one fault block in the southwestern SSR a white unlithified zone at the base of one cooling unit in Trt is designated **Tru**. The unit is labeled **Tr** where the distinction between Trt and Tri is not mappable or has not been made.

White porphyry contains 1-10% 0.2-1 mm quartz, feldspar, and sparse biotite phenocrysts in aphanitic white to light gray matrix. Convoluted parallel layering 3-10 cm thick, interpreted to be a flow foliation, is abundant in Tri at several locations. White to glassy dark brown tuff contains feldspar, quartz, sparse biotite crystals, and variable percentages of clasts in an aphanitic matrix. Clasts include 0.2- to 30-cm long flattened glassy black to dull white pumice clasts displaying wispy ends and 1- to 10-cm diameter, equant, angular feldspar porphyry and aphanitic clasts light in color. Pumice clasts define a pervasive compaction foliation. Tuff exposures include 850-m-thick fault-bounded sections. Other portions of Tr show intrusive relations: contacts with Mesozoic rocks are locally steep and irregular, and a Tr sill several meters wide intrudes TR(?)qt in northwestern n6d. Some steep, irregular contacts and compaction foliation orientations may result from deposition of Tr tuff atop a steep, irregular topography. Similar discontinuous Oligocene tuff units in the Yerington district 75 km to the east onlap pre-ashflow hills (Proffett and Proffett, 1976).

Tr is not metamorphosed or internally deformed, except for the compaction of pumice clasts. Isotopic date sample 4 from Tr near the eastern edge of the map yielded an age of 31.03±0.15 Ma ($^{40}Ar/^{39}Ar$ on sanidine; C. Henry, written commun., 1999). Separate tuffs from the southwestern SSR yielded dates of 24.93±0.06 Ma and 28.74±0.07 Ma (Isotopic date samples 11 and 12; $^{40}Ar/^{39}Ar$ on sanidine; C. Henry, written commun., 2001). A rhyolite dike, apparently Tri, from the Black Eagle Mine in the Rawhide area 4 km west of the southwest corner of the map was dated at 14.7 Ma (K-Ar, Silberman and others, 1975).

Ekren and Byers (1986) mapped Tri in the quadrangle adjacent to the south, as the Miocene rhyolite of Rawhide, Trt southwest of the Nevada Scheelite Camp as the Miocene tuff of Copper Mountain, and Trt south of the Nevada Scheelite Camp as the Oligocene or Miocene tuff of Gabbs Valley. Black and others (1991) tentatively correlated other portions of Tr exposed in this map area as the early Miocene tuff of Arc Dome. C. Henry (written commun., 2001) correlates the tuff at isotopic date sample 11 to one of the tuffs in the tuff of Gabbs Valley of Ekren and Byers (1986).

Tbs — Red feldspar porphyry (Tertiary) Brick-red-weathering feldspar porphyry found in several small exposures primarily near the northwestern rangefront and in the northeast, east of State Highway 839. The porphyry contains distinctive 1 x 4-8 mm to 4 x 4 mm feldspar phenocrysts in an unaltered aphanitic matrix. Vesicles and amygdules 2 cm long are locally common. No internal stratification or definitive intrusive relations were observed.

Tbs is not metamorphosed or internally deformed. Tbs is a pre-31-Ma basaltic andesite map unit mapped in the Slate Mountain Quadrangle to the east by C. Henry (written commun., 1999).

CzMzi — Felsic plutons (Cenozoic and/or Mesozoic) Six pale tan felsic dikes and small plutons mapped northwest, north, and northeast of Big Kasock Mountain and one light- to medium-brown dike 2 km southeast of the Red Ant Mine. Most intrusions consist primarily of 1 mm feldspar crystals, plus quartz and white mica. Dike southwest of Red Ant Mine contains 50% phenocrysts of 2-6 mm hornblende and 1-2 mm feldspar in a medium brown aphanitic matrix. CzMzi plutons are not folded, metamorphosed, or penetratively deformed. CzMzi is Cenozoic and/or Mesozoic in age because unit postdates pre-Late Cretaceous penetrative deformation (D_1) and post-metamorphic deformation (D_2 and D_3). CzMzi plutons are not near Cretaceous granite contacts and thus are not necessarily related to them. One pluton intruded along the Cenozoic fault forming the n6b-n7a boundary apparently postdates the fault, implying that this pluton is Cenozoic.

Kg — Granitoid (Late Cretaceous) Pale pink and white, yellow-brown-weathering granitoid, including aplite and pegmatite, primarily exposed as five large plutons 0.5 km in length. The Sand Springs and Nevada Scheelite plutons are labeled on map. Seven smaller granitoid dikes and plutons are also mapped. Kg crosscuts n1, n2a, n6b, n6c, n7b, n7c, and n7d. Granitoid consists of quartz, orthoclase, untwinned feldspar, biotite, and locally hornblende in 0.1-3 mm crystals. The granite is locally porphyritic; orthoclase phenocrysts range up to 20 mm long. Beal and others (1964) and Schilling (1964) described three composition types within Kg. A porphyritic granite phase, comprising most of the Sand Springs pluton, contains 40-70% potassium feldspar phenocrysts in a groundmass of 40-60% plagioclase feldspar (percentage of groundmass), 25-40% quartz, 5-10% potassium feldspar, 5-10% biotite, 0-1% hornblende, and <1% sphene, apatite, and magnetite. A granodiorite phase exposed in the northwestern portion of the Sand Springs pluton contains 60-70% plagioclase, <10% potassium feldspar, 5-10% quartz, 5-10% hornblende, 1-5% biotite, and <1% sphene, apatite, zircon, and magnetite. A biotite-rich granodiorite phase exposed in the Nevada Scheelite pluton contains 55-65% plagioclase feldspar, 10% potassium feldspar, 15% quartz, 5-15% biotite, and 0-5% hornblende. Kg shows no stratification except 1 km east of the Red Ant Mine where segregations of felsic and mafic minerals are parallel to the pluton contact and at a high angle to S_1. Kg is not metamorphosed or deformed in D_1 or D_2 (see accompanying text for documentation).

Different dating techniques provide a wide range of Late Cretaceous dates from samples located on the map and on figure 1 (table 1). A small granitoid pluton 0.2 km from the northern margin of Sand Springs pluton (fig. 1; 39° 16' N. latitude, 118° 21' W. longitude) is tentatively dated at no younger than ~80 Ma (U-Pb on zircon; table 4; Satterfield and Oldow, 1996). The Sand Springs pluton in the southern Sand Springs Range has been dated at 67±4 Ma, 78±2.0 Ma and 81.7±2.0 Ma (K-Ar on biotite; Schilling, 1964; fig. 1). The Sand Springs pluton has been dated at 81-82 Ma by Rb-Sr (John, 1992). $^{40}Ar/^{39}Ar$ dates of metamorphic rocks flanking the Sand Springs pluton in the map area are also interpreted to be ages of Sand Springs pluton emplacement (see text for documentation). These dates are: 85.47±0.33 Ma (isotopic date sample 1; $^{40}Ar/^{39}Ar$ on hornblende; Satterfield, 1995) and 77 Ma (isotopic date sample 3; $^{40}Ar/^{39}Ar$ on actinolite; Satterfield, 1995). The Nevada Scheelite pluton has been dated at 85.9±3.5 Ma and 89.9±1.0 Ma (K-Ar on biotite; Schilling, 1964; fig. 1) and at ~98 Ma (Rb-Sr; John, 1992). Kg aplite plutons are distinguished from CzMzi aplite plutons by being within 1 km of large granite-granodiorite pluton contacts.

JTRfp — Dark-green feldspar porphyry plutons (Jurassic and/or Triassic) Dark-green feldspar porphyry exposed as nine plutons that crosscut contacts and bedding in the southern portion of the map area. Exposed in n6d, n7c, n7d, and n8, including extensive exposures in the southwestern portion of the map in n7d. Contains 0.5-1 mm plagioclase feldspar phenocrysts and rare, mostly altered olivine(?) phenocrysts in an aphanitic matrix. JTRfp locally is phaneritic, consisting of 0.5-1 mm feldspar and mafic minerals. Rarely contains 2- to 20-mm-thick contorted parallel laminae interpreted to be a flow foliation. Intrusive igneous origin suggested by: a) steep, non-planar, and discontinuous contacts, such as on the southwest flank of Big Kasock Mountain; b) unit crosscuts TR(?)ct-TR(?)qt contacts in n6d; and c) unit crosscuts bedding (S_0) and TR(?)c-TR(?)ct contacts in n7c.

A spaced cleavage (S_1) has been recorded at several locations. Metamorphic minerals include biotite and chlorite.

JTRfp is Jurassic and/or Triassic in age because: a) a JTRfp pluton crosscuts TR(?)ct in n6d; b) JTRfp contains a greenschist metamorphic mineral assemblage consistent with other units metamorphosed and deformed in pre-Late Cretaceous D_1 and unlike Cenozoic igneous rocks which are not metamorphosed; and c) JTRfp is folded in map scale D_1 folds southwest of the Nevada Scheelite pluton. JTRfp predates Cretaceous granitoid emplacement because at least one Cretaceous granitoid dike crosscuts JTRfp adjacent to the JTRfp-Kg contact in the extreme southeast corner of the map and because three mines in the southern SSR exploit mineralization at the Kg-JTRfp contact which apparently formed during Kg intrusion (table 2).

TRqp — White-yellow quartz-feldspar porphyry plutons (Triassic) White to yellow quartz-feldspar porphyry exposed as large sill-like plutons in n6a and also exposed in n3b, n6b, and n6c. Probably the same unit outcrops as two 3- to 4-m-thick sills on the flank of Slate Mountain in the Bell Canyon Quadrangle, adjacent to the Big Kasock Mountain Quadrangle to the northeast (JTRr map unit of Henry, 1996). TRqp consists of 1- to 3-mm quartz and feldspar phenocrysts in an aphanitic quartz-mica matrix. Locally TRqp includes a breccia composed of 5-cm-long tectonically stretched quartz-feldspar porphyry clasts in an igneous quartz-feldspar porphyry matrix. This intraformational breccia is exposed 1 km southeast of Sand Springs Peak. Evidence suggesting intrusive igneous nature includes: a) irregular discontinuous shapes of TRqp exposures; b) inclusions of TRcg and TRc within (the larger ones are mapped); c) several 1- to 4-m-wide dikes and sills of same rock type that extend from mapped contacts into adjacent units 0.2 km northeast of isotopic date sample 3 in n6c and 0.1 km west of isotopic date sample 2 in n6a; and d) an irregular contact which crosscuts TRc-TRcg contacts. TRqp is not stratified.

TRqp contains a penetrative metamorphic foliation (S_1) and locally a stretched clast lineation. TRqp contains metamorphic minerals white mica, quartz, biotite, and chlorite. Sample from location 2 in n6a is tentatively dated at 237±5 Ma (U-Pb on zircon; table 1; Satterfield and Oldow, 1996). TRqp intrudes TRc in n6a and was metamorphosed and folded in pre-Late Cretaceous D_1.

TRfqp — Dark-green quartz-feldspar porphyry plutons (Triassic) Dark-green porphyry exposed as sills in n6a, n3b, and n6c. TRfqp consists of 1- to 3-mm quartz and feldspar phenocrysts in an aphanitic quartz-mica matrix. Unit locally includes a breccia composed of 20-cm-long, tectonically stretched quartz-feldspar porphyry clasts in an igneous quartz-feldspar porphyry matrix.

TRfqp contains a penetrative metamorphic foliation (S_1) and locally a stretched clast lineation. TRfqp contains metamorphic minerals white mica, quartz, biotite, and chlorite. Unit is interpreted to be Triassic because of similarities to dated TRqp. Although similar to TRqp in outcrop pattern, location, and composition, TRfqp is mapped as a separate unit because the striking matrix color difference is typically a sharp and mappable contact.

TRc — Light-gray carbonate rocks (Late Triassic) Light-gray foliated carbonate exposed in n3b, n4, and n6a. TRc consists of elongate calcite crystals typically 0.1-1 mm long. Original bedding is generally not visible. At several locations several centimeter wide bands of rusty brown fossil fragments of 0.5- to 1-cm-thick resistant, dark red laminae define original bedding. TRc is 450 m thick in n6a.

Map unit commonly contains a penetrative metamorphic foliation (S_1) defined by elongate calcite crystals and a closely spaced fracture cleavage (S_1). Structurally higher levels of TRc have yielded an ammonite, *Indojuvavites* cf. *I. angulatus*, characteristic of the late Early Norian Magnus Zone in the Upper Triassic (fossil locality #1 on map; N.J. Silberling, written commun., 1989). TRc is crosscut in n6a by TRqp, which is tentatively dated at 237±5 Ma (isotopic date sample 2; U-Pb on zircon; Satterfield and Oldow, 1996). Carbonate map units are mapped as TRc only where compelling correlations to the dated n6a section can be made.

TRcc — Dark-gray carbonate rocks (Triassic) Dark-gray, sooty carbonate exposed as two thin intervals within TRc in n6a, in the northwestern portion of the map. TRcc consists of equal amounts of 5- to 20-cm-thick limestone flags and interbedded fissile limestone. The structurally lower interval is 0- to 20-m-thick; the upper interval is 50 m thick.

TRcc contains fissility (S_1) at angles to bed boundaries and spaced fracture cleavage (S_1). Unoriented, lath-shaped, scapolite(?) molds ~1 cm long are locally common in limestone flags. This unit is inferred to be Triassic because it is interstratified with TRc, which contains a Triassic ammonite.

TRcg — Felsic volcanogenic conglomerate (Triassic) Light-brown to yellow-white conglomerate commonly containing a component of 1-mm quartz grains. TRcg is exposed in n3b, n4, and n6a. Tectonically stretched clasts, 2-35 cm long, include light-brown and pale-yellow feldspar porphyry, similar-colored aphanitic rock fragments, rare quartz porphyry, and sparse dark-gray slate clasts in a quartz-feldspar sandstone matrix. Sparse dark-gray slate and carbonate interbeds include 5 m dark-gray slate in n3b. A limestone conglomerate composed of 30- to 50-cm-long carbonate blocks in a brown sandstone matrix is found at the base of TRcg in n6a. Otherwise, no bedding observed within this unit. TRcg is ~120 m thick in n6a.

TRcg displays a penetrative metamorphic foliation (S_1) and stretching lineation. Metamorphic minerals in volcanogenic conglomerate include biotite, white mica, chlorite, and quartz. Constraints supporting a Triassic age are: a) in depositional contact with TRc, which contains a Late Triassic fossil in its upper part; and b) crosscut by TRqp, dated at 237±5 Ma (Satterfield and Oldow, 1996).

TRa — Dark gray slate (Triassic) Medium- to dark-gray slate interstratified with silty carbonate beds mapped in two small areas in n3b and n6a. Bedding defined by 1-2 mm tan, silty parallel laminations and 15- to 20-cm to 1 m-thick carbonate beds. TRa is 20 m thick in n6a.

TRa displays a penetrative metamorphic foliation (S_1) and fissility (S_1). Locally TRa contains metamorphic andalusite and actinolite porphyroblasts. Inferred to be Triassic because in same stratigraphic succession in n6a as TRc, which contains a Triassic ammonite.

TR(?)c — Carbonate rocks (Triassic?) Light gray fossiliferous, foliated limestone exposed only in core of one syncline in n7c. Commonly contains several millimeter-long fossil fragments, including echinoderm fragments. TR(?)c is 25 m thick in n7c.

TR(?)c contains a penetrative metamorphic foliation (S_1) defined by elongate calcite crystals. Inferred to be Triassic(?) because gradationally overlies TR(?)ct which contains fossils possibly indicative of a Triassic age. Possibly correlative to TRc since rock types are similar. However the stratigraphic succession containing TRc in n6a is unlike the succession in n7c containing TR(?)c (fig. 3) which does not support this correlation.

TR(?)ct — Carbonate rocks and tuff (Late Triassic?) Brown-weathering, locally gray-weathering carbonate and interstratified white, light gray, and dark gray crystal-lithic and crystal tuff metamorphosed to slate. TR(?)ct is extensively exposed in n6d and n7c. Carbonate rocks include sparse limestone conglomerate beds containing flattened clasts 40- to 50-cm-long. Elsewhere, at several localities carbonate contains abundant 1- to 10-mm echinoderm and 0.5- to 5-cm bivalve fragments. Some bivalve fossils have both valves attached. Mostly aphanitic tuff contains sparse feldspar phenocrysts and rare accretionary lapilli. Tuff and limestone beds are 30 cm to >3 m thick and locally graded in n7c, providing facing indicators plotted on map. Bedding also defined by 1- to 20-mm-thick brown laminae and beds within gray limestone. TR(?)ct is 200 m thick in n7c.

TR(?)ct contains a penetrative metamorphic foliation (S_1) and slaty cleavage (S_1). Tuff contains metamorphic minerals biotite, white mica, and graphite. Late Triassic(?) age inferred from possible megalodontid bivalve fossils at fossil localities 2 and 3 in n6d. Megalodontid bivalves are only known from Upper Triassic rocks (N.J. Silberling, written commun., 1991). Fossils are randomly oriented and not in growth position. Near State Highway 839 this unit contains Halorella-like brachiopods which suggest a Triassic rather than Jurassic age (Banaszak, 1969).

TR(?)qt — Lithic-crystal tuff (Triassic?) White, light gray, light brown, dark green, and dark gray lithic-crystal tuff, interstratified crystal tuff, and rare carbonate interbeds. TR(?)qt is exposed in n6d, n6f, n7c, and n8. Lithic-crystal tuff contains trace amounts to 90% aphanitic dark gray to grayish white clasts several cm long, displaying wispy ends. The matrix consists of 1-2 mm quartz and feldspar crystals in an aphanitic matrix. Crystal tuff typically appears as a slate, as does crystal tuff in TR(?)ct. Crystal tuff is identical to matrix of lithic-crystal tuff, and locally includes a feldspar porphyry consisting of euhedral feldspar in a dark green, aphanitic matrix. Bedding defined by bed boundaries between lithic crystal tuff and crystal tuff. Bedding is not preserved within tuff or carbonate beds, which are on the order of one to several meters thick. TR(?)qt is 75 m thick in n7c.

TR(?)qt displays a penetrative metamorphic foliation and slaty cleavage(S_1). Crystal tuff and crystal-lithic tuff contain metamorphic minerals biotite, white mica, chlorite, and quartz. Triassic(?) age of unit is inferred from age of TR(?)ct which is in depositional contact with TR(?)qt in n7c.

MzPzfp — Dark-green feldspar porphyry pluton (Mesozoic and/or Paleozoic) Dark-green feldspar porphyry exposed as a single pluton within n6c. MzPzfp contains 0.1-mm feldspar phenocrysts within an aphanitic matrix. The matrix displays a primary, non-tectonic alignment of microscopic feldspar crystals (pilotaxitic texture). The irregularity and steepness of the the MzPzfp-MzPzc contact and the observation that the MzPzfp body is completely surrounded by MzPzc suggest that MzPzfp is an intrusive rock.

Locally MzPzfp contains spaced cleavage (S_1). Metamorphic biotite clots have replaced possible mafic phenocryst minerals. Biotite is not necessarily syn-D_1. Age of MzPzfp is constrained to be Mesozoic and/or Paleozoic because pluton intruded MzPzc and was deformed in pre-Late Cretaceous D_1. MzPzfp is distinguished from JTRfp by the smaller size of feldspar phenocrysts and pilotaxitic texture of MzPzfp.

MzPzf — Felsite intrusive rocks (Mesozoic and/or Paleozoic) Yellow to white intrusive igneous rock exposed over large areas in n6c, n7c, and n7d. Contains 1- to 2-mm feldspar phenocrysts that are difficult to recognize in hand sample within an aphanitic matrix. Large carbonate inclusions 0.2 km long and possibly as long as 0.5 km are present in n7c and n7d. Inclusion boundaries are difficult to recognize and typically not mappable; one is mapped on the south flank of Big Kasock Mountain in n7d. Also indicating an intrusive nature are contacts that cross-cut the MzPzc-MzPzav contact south of Big Kasock Mountain in n7d and irregular MzPzf-MzPzc contacts in n7d and n7c. MzPzf lacks internal stratification.

MzPzf typically shows a fracture cleavage (S_1). Matrix contains the metamorphic minerals chlorite and white mica. Age constrained to be Mesozoic and/or Paleozoic because MzPzf is deformed in pre-Late Cretaceous D_1 and intruded MzPzc and MzPzav.

MzPzcs — Schist and carbonate rocks (Mesozoic and/or Paleozoic) White, yellow, green, and brown actinolite-biotite schist interstratified with gray, yellow, and dark-green carbonate conglomerate and gray, yellow, and dark-brown structureless carbonate exposed in several small areas in the northwestern portion of n6c. Schist layers contain 1- to 3-mm actinolite porphyroblasts. Schist protolith is not known. Carbonate layers contain 3 cm to 1 m-long tectonically flattened and stretched light-colored carbonate clasts in a carbonate matrix. Bedding is not preserved. Individual schist and carbonate layers are typically 3 cm to 9 m thick. MzPzcs is 100 m thick.

Carbonate and schist display a penetrative metamorphic foliation and fissility (S_1). Actinolite porphyroblasts are foliated and locally lineated. Flattened carbonate clasts also define S_1. Schist at isotopic date sample 3 contains metamorphic minerals actinolite, biotite, chlorite, quartz, and calcite. Other schist samples also contain white mica and feldspar. MzPzcs is constrained to be older than 77 Ma, the $^{40}Ar/^{39}Ar$ date on actinolite at sample location 3. The 77-Ma date is interpreted to be the age of intrusion of Cretaceous plutons (Kg), not the age of the metamorphism of the schist or the crystallization age of the schist protolith. Field relations show syn-D_1 metamorphism predated Cretaceous plutons (see accompanying text).

MzPzc — Carbonate rocks (Mesozoic and/or Paleozoic) White, light-gray, and dark-gray foliated and locally banded carbonate extensively exposed in n1, n2b, and n7d. MzPzc also exposed in n2b and n3a. Typically completely metamorphosed to foliated marble consisting of elongate calcite crystals 0.2- to 0.3-mm-long. In n7d west of the Nevada Scheelite pluton (fossil locality 4), in n7d east of Big Kasock Mountain and State Highway 839, and in the northern portion of n6c, MzPzc contains abundant bivalve, gastropod, and echinoderm fragments 1- to 30-mm-long. In the same part of the range, MzPzc contains crinoid and bryozoan fragments of in-determinate age (C. Stevens, written commun. to H.J. Brown, Pluess-Staufer Inc., 1994). MzPzc includes rare carbonate conglomerate consisting of 4-cm-long tectonically stretched clasts in a light gray carbonate matrix. Original bedding is locally preserved as 0.5- to 1.5-m-thick resistant benches continuous locally up to 50 m and visible on aerial photographs. MzPzc also locally contains several-mm-thick white calcite stringers in dark gray carbonate. Mapped MzPzc units range in thickness from 20 to several hundred meters.

Elongate calcite crystals define a metamorphic foliation (S_1). This foliation and parallel fissility (S_1) is not pervasive throughout the map area. In a broad zone 1 km wide west of the Nevada Scheelite pluton foliated marble is replaced by white unfoliated marble consisting of coarse, 1 mm, unoriented calcite crystals. Age of MzPzc is constrained to be Mesozoic and/or Paleozoic because unit predates pre-Late Cretaceous D_1. MzPzc could be at least partly equivalent to similar-appearing TR(?)c and/or TRc. Carbonate rocks are mapped as MzPzc where compelling rock type, fossil, or stratigraphic succession correlations to TR(?)c or TRc do not exist. Unlike TR(?)c, MzPzc units are not interstratified with or in depositional contact with quartz-bearing tuff. Unlike TRc, MzPzc units are not in contact with quartz-bearing volcanogenic conglomerate. Different MzPzc map units in different fault blocks are not necessarily correlative.

MzPzsl — Black slate (Mesozoic and/or Paleozoic) Dark-gray to black non-calcareous slate containing sparse interbeds of feldspathic sandstone, lithic-crystal tuff, and carbonate mapped only in two areas in n6c. Tuff and sandstone interbeds are similar in appearance: both contain varying amounts of 1- to 10-mm-long aphanitic black clasts, some flattened with wispy ends and others equant and rounded. Tuff and sandstone typically contain abundant 0.1- to 1-mm feldspar grains or crystals and trace amounts of quartz and chert within varying amounts of aphanitic, dark gray matrix. Chert grains may be silicified volcanic rock fragments. Beds containing euhedral feldspar crystals, abundant matrix, and wispy, flattened clasts are interpreted to be tuff. Beds containing little matrix and rounded grains are interpreted to be sandstone. Sandstone and tuff beds are 5- to 10-cm-thick. Silty laminations are locally present in slate. Overall thickness of MzPzsl is 100 m.

Fissility in slate defines a tectonic foliation (S_1). Flattened and locally stretched clasts in tuff define a foliation (S_1) and lineation. Chlorite is the syn-D_1 metamorphic mineral in sandstone and tuff. MzPzsl is Mesozoic or Paleozoic in age because it predates pre-Late Cretaceous D_1. Mapped as a separate unit from MzPzas, which is similar in appearance, because MzPzsl lacks andalusite porphyroblasts, contains tuff and sandstone interbeds different in composition from interbeds in MzPzas, and clastic interbeds in MzPzsl contain only trace amounts of quartz, unlike quartz-rich interbeds in MzPzas.

MzPzvs ($MzPzvs_4$, $MzPzvs_3$, $MzPzvs_2$, $MzPzvs_1$) — Volcanogenic sandstone, mudstone, and conglomerate (Mesozoic and/or Paleozoic) Tan to dark-brown feldspathic sandstone and conglomerate beds intercalated in light to dark brown mudstone comprise the only map unit in large n6b and n7b. MzPzvs includes rare, several-meter-thick carbonate interbeds. Sandstone beds are composed of 0.1- to 2-mm plagioclase feldspar, untwinned feldspar, and small amounts of volcanic rock fragments in abundant mica-rich matrix. Tan and medium brown pebbles and cobbles consist of 1- to 20-cm-long, tectonically stretched feldspar porphyry, mudstone, and rare sandstone clasts. Bedding is commonly preserved: sandstone and conglomerate beds are 5 cm to several meters thick and locally contain parallel and convolute laminations, graded beds, cross-laminations, and load casts. Four subunits comprising a stratigraphic succession of known facing are mapped in n7b: **$MzPzvs_4$** Mudstone and subordinate amounts of sandstone, 50 m thick. **$MzPzvs_3$** Sandstone, 100 m thick. **$MzPzvs_2$** Mudstone and subordinate amounts of sandstone, 75 m thick. **$MzPzvs_1$** Sandstone, 75 m thick.

MzPzvs contains a penetrative metamorphic foliation (S_1) and fissility (S_1) that is pervasive throughout n7c and the northern part of n6c. Clasts are commonly stretched, defining a lineation. Unit contains metamorphic chlorite, biotite, and green amphibole. Tabular green amphibole porphyroblasts are 2 mm long. Only age constraint on MzPzvs is that it is deformed in pre-Late Cretaceous D_1. Quartz grains are almost completely lacking in MzPzvs, distinguishing sandstone and conglomerate beds in this unit from coarse clastic beds in other volcanogenic units such as TRcg, TR(?)qt, MzPzsl, and MzPzas.

MzPzas — Andalusite schist (Mesozoic and/or Paleozoic) Black to silver-gray slate and schist typically containing andalusite porphyroblasts. Subordinate amounts of yellow- to brown-weathering quartzose volcanogenic rocks and light brown, white to gray, foliated carbonate rocks are interstratified. MzPzas is extensively exposed in n1 and n3a and is also found in small n2b and n5. Sandstone contains 1- to 2-mm grains of abundant quartz, chert, and feldspar. Conglomerate or lithic tuff is composed of 0.5- to 8-cm-long, tectonically stretched aphanitic dark-gray, light-gray, tan, and white chert clasts in a quartz-feldspar sandstone matrix. Chert clasts are possible silicified volcanic rock fragments. Sandstone, conglomerate or tuff, and carbonate beds intercalated in black schist range in thickness from 8 cm to 3 m. Bedding is rarely preserved as light-brown, 1- to 20-mm-thick silty laminae and beds in sandstone and andalusite schist. MzPzas protolith is organic-rich shale. MzPzas is 60 m thick in n1, 80 m thick in n3a, and 30 m thick in n2b.

Andalusite schist and intercalated beds contain a penetrative metamorphic foliation (S_1) and fissility (S_1). Up to 5-cm-long andalusite phorphyroblasts are typically foliated (S_1) and locally lineated. Stretched clasts in conglomerate also define a lineation. Andalusite schist samples generally contain the metamorphic minerals andalusite, biotite, white mica, graphite, and quartz. Chlorite, amphibole, chloritoid, and garnet are also present in some andalusite schist samples. Intercalated volcanogenic clastic rocks commonly contain the metamorphic minerals biotite, chlorite, white mica, and quartz. Some volcanogenic clastic rocks also contain garnet or chloritoid. Only age constraint on MzPzas is that it is deformed in pre-Late Cretaceous D_1. Compelling correlations between MzPzas sections in different nappes do not exist. MzPzas differs from MzPzvs, MzPzsl, and TRa in that it contains quartz-rich clastic interbeds, and because relatively thick stratigraphic successions in n3a and n1 that include MzPzas are not correlative to thick successions in n6b, n6c, and n6a (fig. 3).

MzPzac — Andalusite schist and carbonate rocks (Mesozoic and/or Paleozoic) Interstratified dark gray andalusite schist and light brown to gray to white foliated carbonate beds. Also interstratified are smaller amounts of yellow-orange to light brown quartz-rich volcanogenic sandstone and conglomerate, gray to light brown felsic schist, and rare dark green feldspar porphyry. MzPzac is mapped in the northern part of the map area within n1 and n3a. Andalusite schist, carbonate, sandstone, and conglomerate in MzPzac are indistinguishable from those in MzPzas described above. Felsic schist in MzPzac consists of 0.05- to 5-mm, typically 0.1- to 0.2-mm crystals. Beds or segregations of each rock type are typically one to several meters thick. Thicker carbonate layers interstratified with MzPzac are mapped as MzPzc. MzPzac is 370 m thick in n1.

MzPzac contains a penetrative metamorphic foliation and fissility (S_1) throughout. Andalusite long axes in andalusite schist and biotite clots in felsic schist define a mineral lineation. Stretched clasts in conglomerate also define a lineation. Conglomerate and sandstone contain pre- or syn-D_1 metamorphic minerals which include feldspar, diopside, quartz, white mica, biotite, chlorite, garnet, amphibole, and epidote. Some tremolite and diopside crystals crosscut S_1. Only age constraint on MzPzac is that it is deformed in pre-Late Cretaceous D_1. MzPzac is distinguished from MzPzas by a higher ratio of carbonate rocks to andalusite schist, and by the presence of additional rock types, including felsic schist, in MzPzac.

MzPzs — Felsic schist and carbonate rocks (Mesozoic and/or Paleozoic) Interstratified white to light-gray foliated carbonate and yellow-white, speckled light-gray schist exposed in small areas of n1. Rock types and bed thicknesses in MzPzs are similar to MzPzac. The protolith of schist in MzPzs is unknown. MzPzs is 100 m thick.

MzPzs contains a pervasive metamorphic foliation and fissility (S_1), and locally a biotite mineral lineation and a stretched clast lineation. Schist contains metamorphic biotite, chlorite, white mica, plagioclase feldspar, calcite, and quartz. The only age constraint on MzPzs is that it is deformed in pre-Late Cretaceous D_1. The small proportion of dark-gray andalusite schist in MzPzs distinguishes this unit from MzPzac and MzPzas.

MzPzhc — Hornblende-biotite schist (Mesozoic and/or Paleozoic) Gray to brown to black hornblende-biotite-quartz schist containing igneous clasts interstratified with subordinate amounts of dark brown slate and sparse carbonate and calcsilicate segregations. MzPzhc is extensively exposed in n2a and also exposed in small areas in the northeastern margin of the map area. Rocks of similar protolith and metamorphic mineral assemblage are exposed on the east flanks of Slate Mountain in the Slate Mountain and Bell Canyon Quadrangles, adjacent to the east and northeast (Henry, 1996). Crystals are commonly 0.1- to 0.5-mm-long and hornblende crystals include porphyroblasts 1- to 10-mm-long. Feldspar and quartz grains or crystals are recognizable porphyroclasts. MzPzhc contains widely variable amounts of greatly tectonically stretched, 10- to 40-cm-long clasts. Clast types include: a) white speckled coarsely crystalline feldspar-amphibole and feldspar-biotite rock; b) pale yellow, light gray, and medium to dark brown feldspar porphyry, feldpar-amphibole porphyry and aphanitic rock; and c) rare brown laminated, chip-shaped mudstone. Bedding is sparsely preserved as parallel laminations within slate intervals. Conglomerate and slate intervals are typically several meters thick. The MzPzhc protoliths may be igneous or sedimentary. MzPzhc is 160 m thick in n2a.

A penetrative metamorphic foliation and fissility define S_1. Stretched clasts and oriented hornblende and biotite crystals define lineations. Schist contains abundant metamorphic biotite and hornblende plus metamorphic actinolite, biotite, epidote, chlorite, quartz, and calcite. Only age constraint on MzPzhc is that it is deformed in pre-Late Cretaceous D_1. Unlike similar-appearing dark-colored volcanic or volcanogenic map units such as MzPzvs and MzPzav, MzPzhc contains abundant quartz and larger metamorphic mineral crystals.

MzPzha — Slate and hornblende-biotite schist (Mesozoic and/or Paleozoic) Dark-brown to olive-green slate and subordinate intercalated gray to brown to black hornblende-biotite-quartz schist extensively exposed in n2a. MzPzha contains the same rock types as MzPzhc. Recognizable beds in MzPzha include 1-cm to 0.5-m layers of parallel laminated siltstone and sandstone interstratified in slate. MzPzha is overall 360 m thick.

A penetrative metamorphic foliation and fissility define S_1. Stretched clasts and oriented hornblende and biotite crystals define lineations. Schist contains metamorphic biotite, hornblende, and quartz. Only age constraint on MzPzha is that it is deformed in pre-Late Cretaceous D_1. MzPzha is distinguished from MzPzhc by containing mostly slate. MzPzha-MzPzhc contacts are apparently gradational and approximately located.

MzPzav — Volcanic conglomerate (Mesozoic and/or Paleozoic) Dark-green-brown volcanic and volcanogenic conglomerate interstratified with lesser amounts of feldspathic sandstone and dark-green feldspar porphyry. MzPzav is exposed in n7a and n7d, primarily on the north and south flanks of Big Kasock Mountain. A thin shale interval is at the structural top of MzPzav, at the MzPzav-MzPzc contact in n7d. Conglomerate contains variable amounts of slightly tectonically stretched, typically slightly rounded, 1- to 5-cm-long clasts. Clasts of dark-green, dark-brown, and yellow feldspar porphyry, feldspar-amphibole porphyry, mudstone chip, and rare carbonate rock are within a feldspathic sandstone or feldspar porphyry matrix. Matrix consists of 0.5- to 2-mm plagioclase feldspar grains or crystals and sparse amphibole crystals or grains. Feldspathic sandstone is difficult to distinguish from feldspar porphyry in MzPzav. Feldspathic sandstone is composed of 80% slightly rounded feldspar grains, while feldspar porphyry is composed of euhedral feldspar grains floating in abundant dark green aphanitic matrix. Beds range in thickness from 15 cm to 2 m and locally contain parallel and convoluted laminations. MzPzav is 275 m thick in n7a and 1000 m thick in n7d.

A metamorphic foliation (S_1) and spaced fracture cleavage (S_1) is common but not pervasive in MzPzav. Slightly stretched clasts provide rare measurable stretched clast lineations. Conglomerate and feldspar porphyry contain metamorphic chlorite, biotite, and white mica. Only age constraint on MzPzav is that it is deformed in pre-Late Cretaceous D_1. MzPzav contains a much larger proportion of conglomerate and igneous feldspar porphyry than MzPzvs. Unlike JTRfp, MzPzav porphyry contains amphibole phenocrysts. MzPzav is distinguished from MzPzhc by the lack of quartz in MzPzav sandstone and conglomerate.

MzPzsg — Shale-chip conglomerate (Mesozoic and/or Paleozoic) Light-brown conglomerate and interstratified feldspathic sandstone exposed only in n7a, on the north flank of Big Kasock Mountain. Conglomerate clasts are dominantly tectonically stretched or oriented, 1-mm- to several-centimeters-long brown shale chips. Feldspathic sandstone consists of feldspar and volcanic rock fragments in mica-rich matrix. Beds include a 15-cm-thick sandstone bed and are commonly parallel laminated and rarely graded. Overall thickness of MzPzsg is 50 m.

Locally MzPzsg displays a metamorphic foliation (S_1), spaced fracture cleavage (S_1), and a stretched clast lineation. Sandstone in MzPzsg contains metamorphic biotite and chlorite. Only age constraint on MzPzsg is that it is deformed in pre-Late Cretaceous D_1.

See accompanying text for references, tables, figures, and a discussion of the geology of the Southern Sand Springs Range.

Field studies in the southern Sand Springs Range were conducted in 1988-2002.

Office review by: Christopher D. Henry (NBMG), Norman Silberling (USGS), and Sandra J. Wyld (University of Georgia).
Field review by: Christopher D. Henry (NBMG).

First edition, first printing, 2002
Printed by Nevada Bureau of Mines and Geology, Reno, Nevada
Edited by Dick Meeuwig; cartography by Robert Chaney

Geologic mapping supported by: Geological Society of Nevada, Arco Oil and Gas Company, the American Association of Petroleum Geologists, the Geological Society of America, Sigma Xi, Rice University, San Jacinto College, and the National Science Foundation (grants to J.S. Oldow).

Nevada Bureau of Mines and Geology
University of Nevada, Mail Stop 178
Reno, Nevada 89557-0088
(775) 784-6691, ext. 2
www.nbmg.unr.edu; nbmgsales@unr.edu